



CrownBio
CONNECTING SCIENCE TO PATIENTS

Corporate Headquarters:

3375 Scott Blvd., Suite 108
Santa Clara, CA 95054

Tel: 855.827.6968
Fax: 888.882.4881

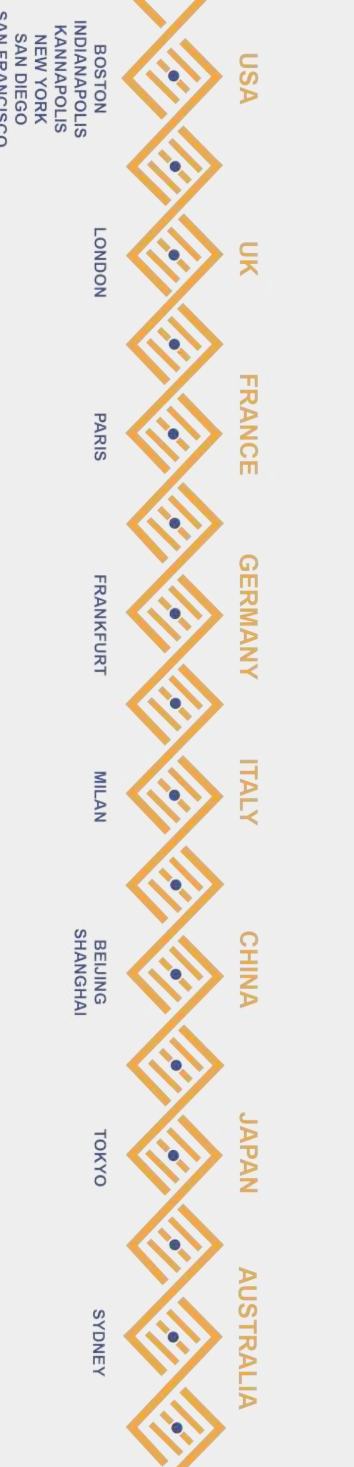
www.crownbio.com

Tumour heterogeneity and combination strategies

Rajendra Kumari, CBUK Ltd

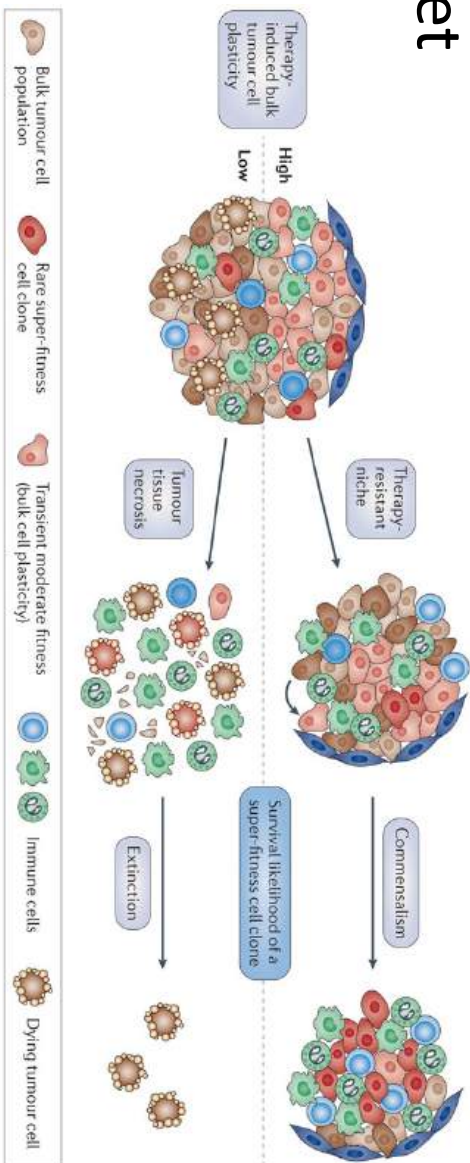
BOSTON
INDIANAPOLIS
KANNAPOULIS
NEW YORK
SAN DIEGO
SAN FRANCISCO

USA
UK
FRANCE
GERMANY
ITALY
CHINA
JAPAN
AUSTRALIA
LONDON
PARIS
FRANKFURT
MILAN
SHANGHAI
TOKYO
SYDNEY



Contents

- Tumour antigen heterogeneity and mutational load influences antitumour immune response
- Importance of tumour antigens in triggering antitumour immune response
- Immuno phenotyping of mouse models
- Human target



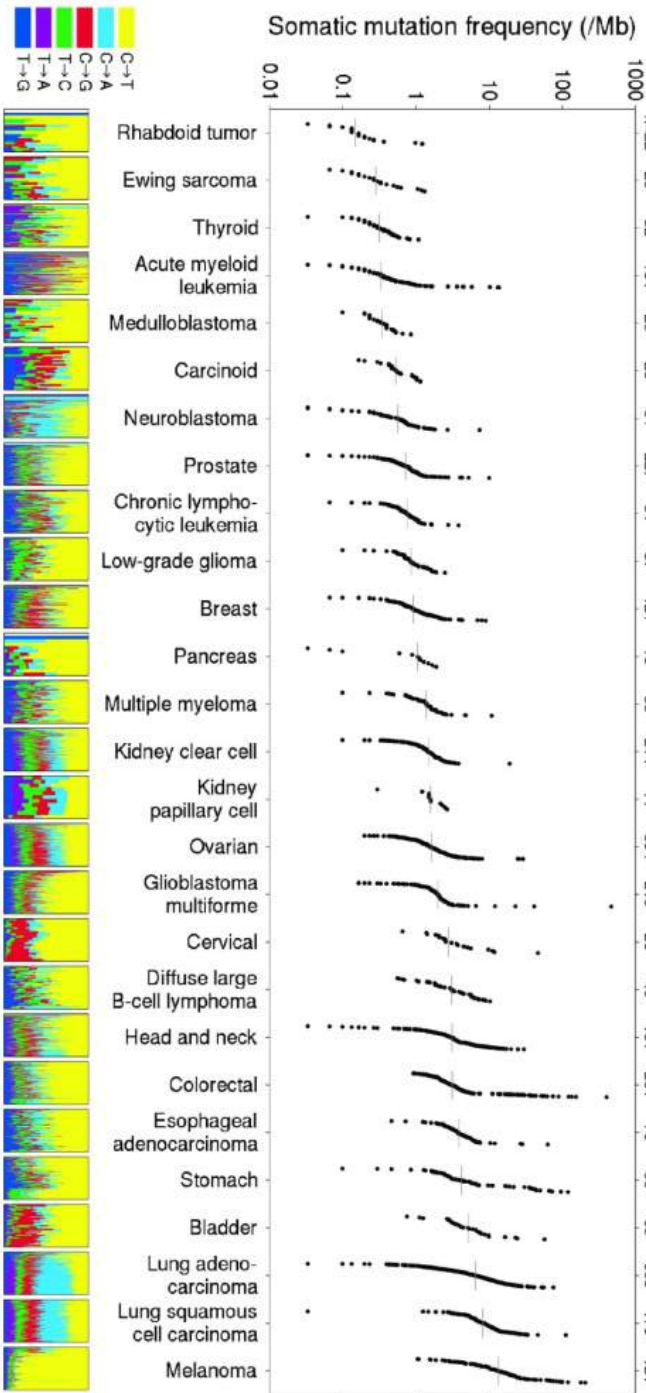
Plasticity of tumour and immune cells: a source of heterogeneity and a cause for therapy resistance?

Michael Hözel, Anton Bovier & Thomas Tütting. Nature Reviews Cancer 13, 365-376 (May 2013)

12/06/16

Mutational heterogeneity in cancer

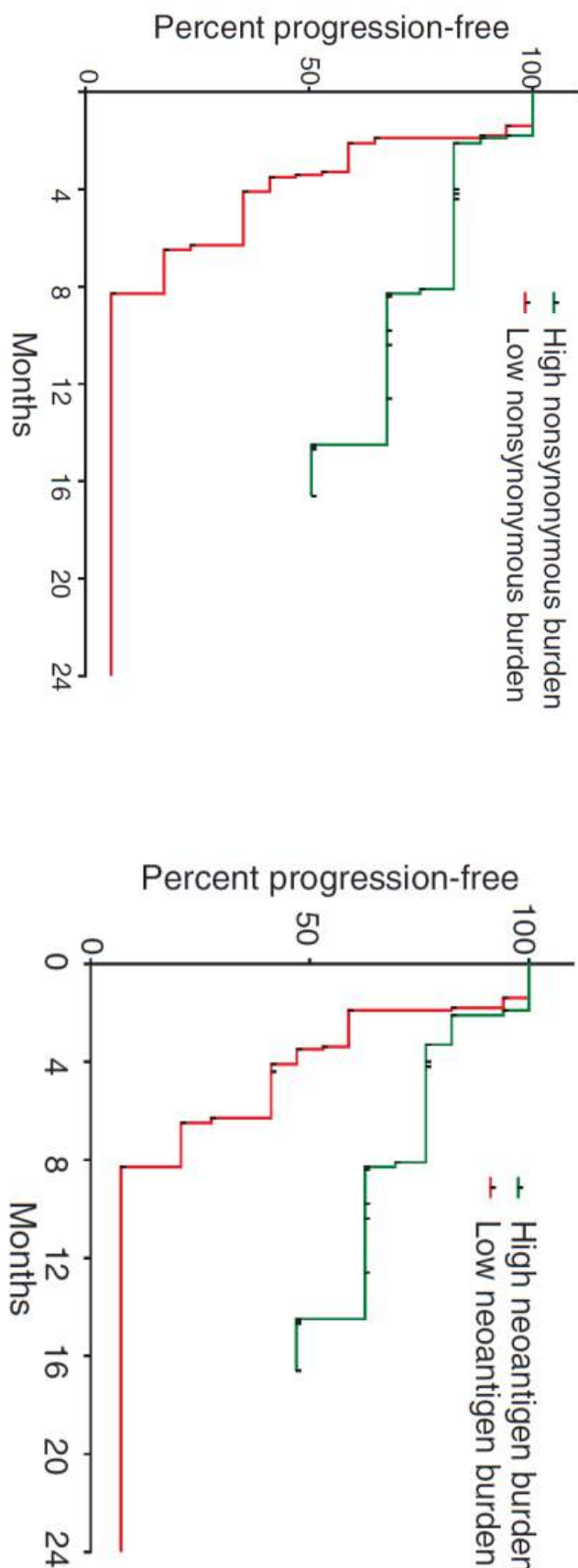
- Neoantigens: nonsynonymous somatic variations acquired by tumours
- Tumours with mutational burden potentially harbour immunogenic antigens resulting in antigens that trigger an anti-tumour immune response e.g. melanoma and lung
- Carcinogens e.g. tobacco, UV and DNA mismatch repair have high mutations
- Establish predictive biomarkers



Lawrence et al; Nature. 2013 July 11; 499(7457):

Mutation mediated sensitivity to PD-1 blockade in NSCLC

- Correlation between neoantigens and mutations
- Both high nonsynonymous mutational and neoantigen burdens are associated with antitumour immune response and clinical response to checkpoint inhibitors
- Genomic landscape shapes the response to anti-PD-1 therapy



Rizvi et al *Science* 2015, 348: 124-128



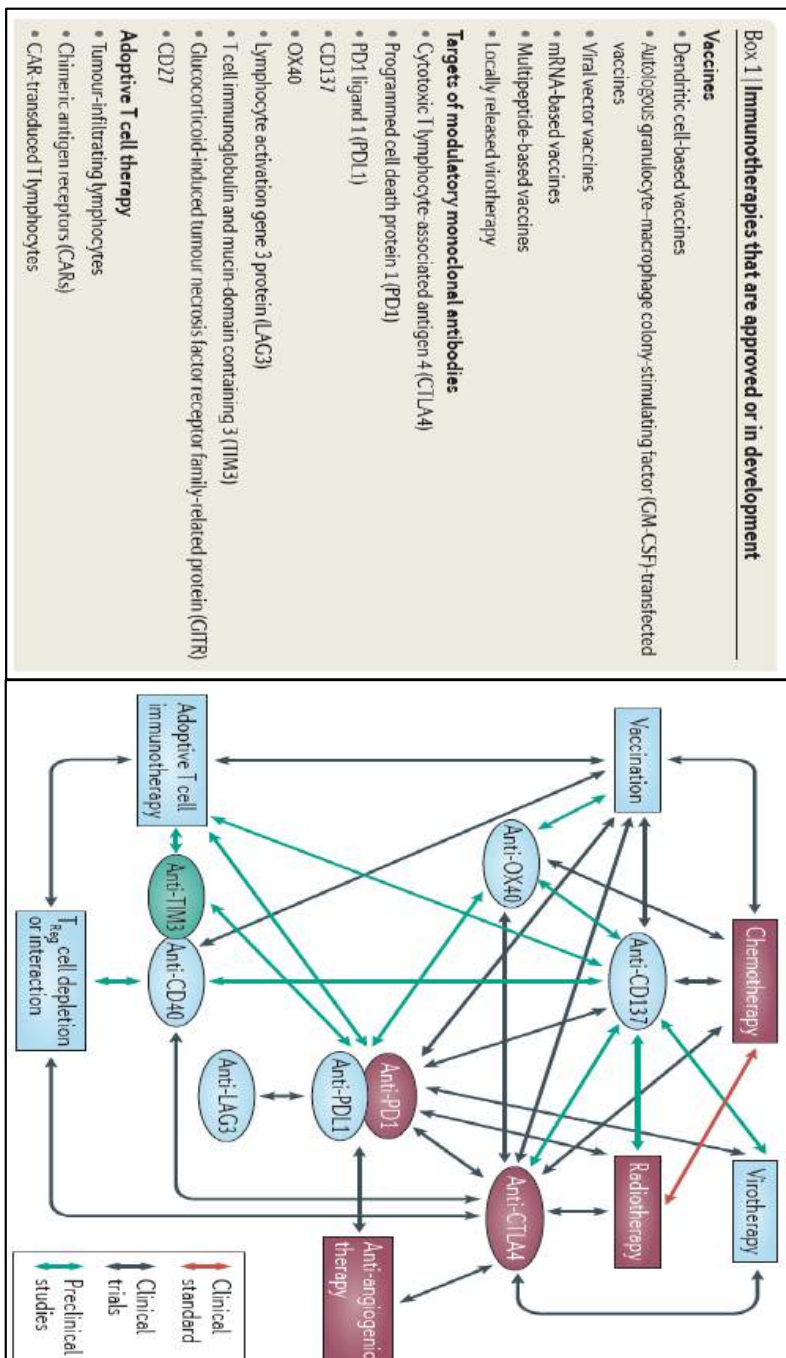
Inducing Immunogenicity

- High burden of clonal neoantigens (i.e. present in all tumour cells) is associated with improved patient survival and durable response to immunotherapy (*Clonal neoantigens elicit T cell immunoreactivity and sensitivity to immune checkpoint blockade*. McGranahan Science 2016)
- Most mutations however occur early on
- Treatment of cancer can induce antigen expression (*Combining immunotherapy and targeted therapies in cancer treatment*. Vanneman & Dranoff, Nature Rev Cancer 2013, 12:237-251)
- Induction of immunogenic cell death can increase antigen presentation to T cells (*Immunogenic Cell Death in Cancer Therapy*. Kroemer et al Annu. Rev. Immunol. 2013. 31:51–72)
- Low mutation load, biomarkers, individualised?

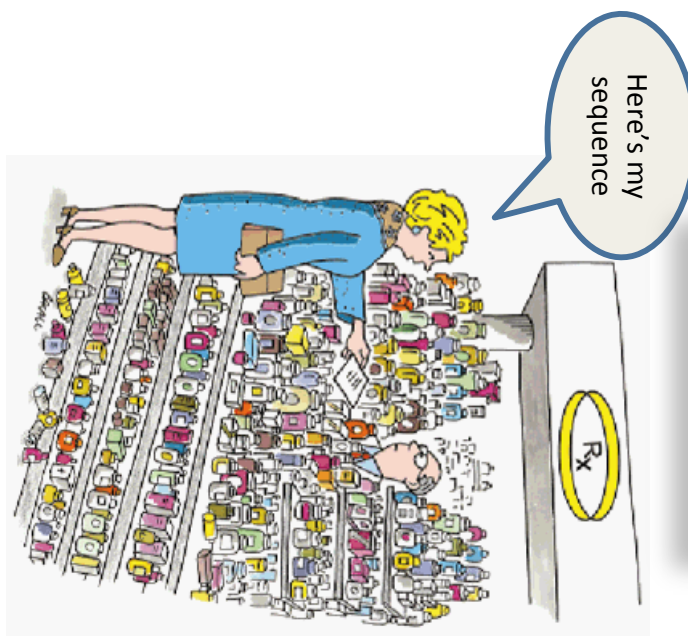
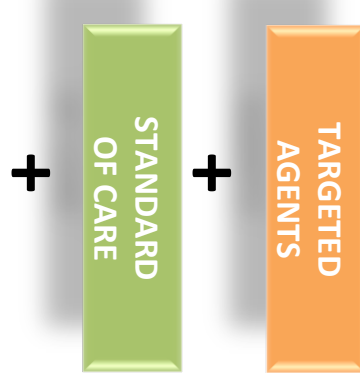


CrownBio
CONNECTING SCIENCE TO PATIENTS

- Opportunities for synergy through rational design
- TME, heterogeneity & resistance needs to be well studied
- Modulation of the immune microenvironment
- Optimisation of dose, sequence and timing, toxicity
- Personalised approach



Smart Combinations



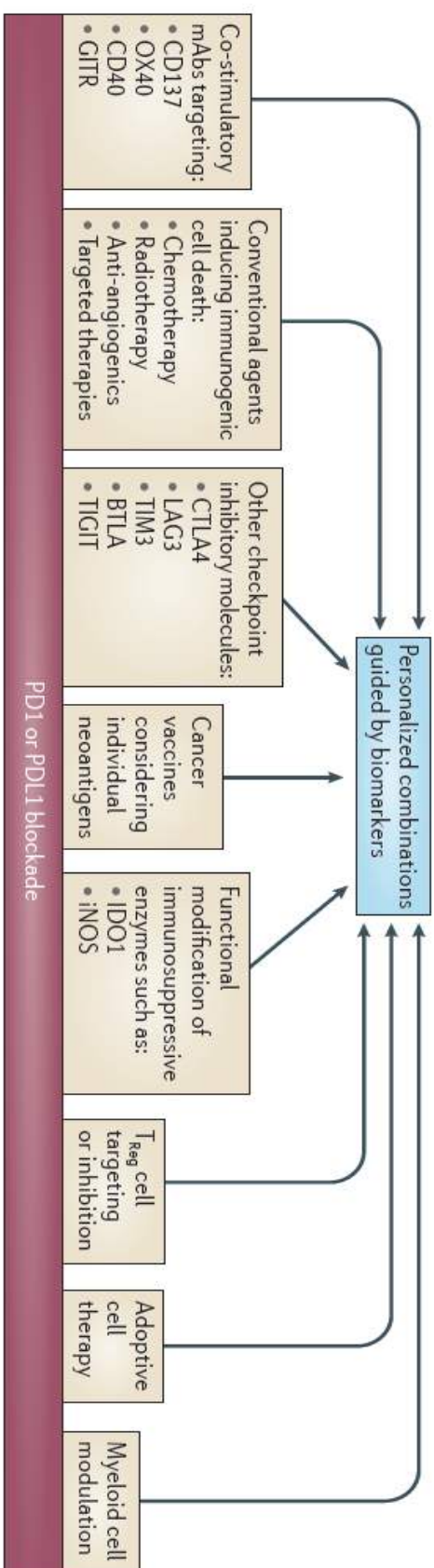
Combinations in the clinic

Breast cancer

- PIII Pembrolizumab v Chemo mTNBC
- PIII margetuximab + Herceptin + chemo mHer2-
- PII Pembrolizumab + HDACi
- PII Durvalumab + tremelimumab
mTNBC or mHER2-
- PII T cell therapy targeting NY-ESO-1 + DC vaccine
- DC + androgen ablation

Prostate Cancer

- PIII Ipi + LIR mCRPC
- PII Provenge + Indoximod refractory adv PC





CrownBio
CONNECTING SCIENCE TO PATIENTS

Murine Models

- Syngeneic-Efficacy/PD
- MuPrime

Global I/O Platform Technologies

CrownBio
CONNECTING SCIENCE TO PATIENTS

- I/O CAR-T
- MiXeno
- PDX

- Advanced I/O
- HuGEMM
- HSC-PDX



CrownBio
CONNECTING SCIENCE TO PATIENTS

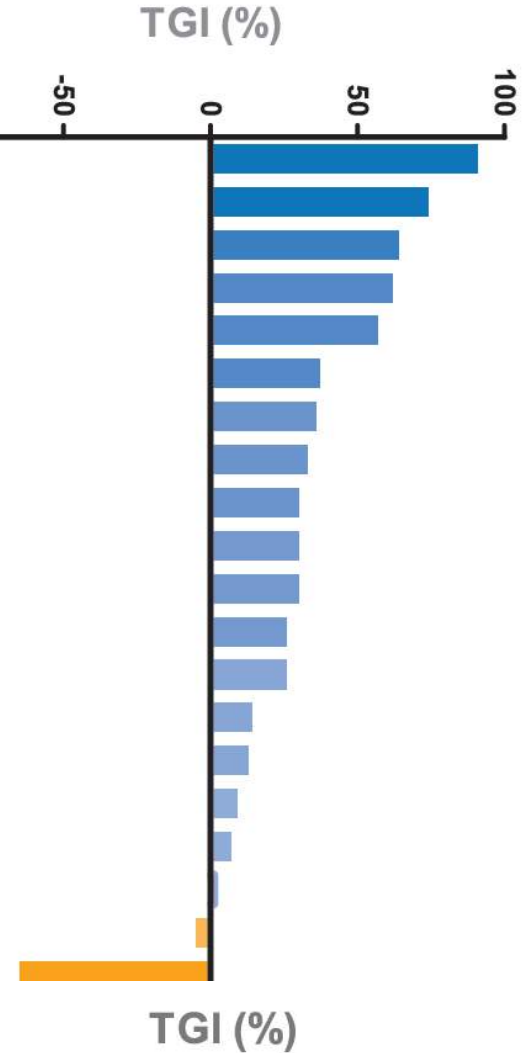
Characterization & Immunophenotyping

| Cancer Type | Cell line | Model type | Mouse Strain | Immune Cell Profiling | RNAseq | Anti-PD-1 | Anti-PD-L1 | Anti-CTLA-4 |
|-------------------|-----------|-----------------|--------------|-----------------------|---------|------------|------------|-------------|
| Bladder cancer | MBT-2 | s.c. | C3H | Yes | Ongoing | Yes | Yes | Yes |
| | 4T1 | s.c./ortho/mets | BALB/c | Yes | Yes | Yes | Yes | Yes |
| Breast cancer | EMT 6 | s.c./ortho | BALB/c | Yes | Ongoing | Yes (s.c.) | Yes (s.c.) | Yes (s.c.) |
| | JC | s.c. | BALB/c | Ongoing | Ongoing | Ongoing | Ongoing | Ongoing |
| Colon cancer | Colon 26 | s.c. | BALB/c | Ongoing | Ongoing | Ongoing | Ongoing | Ongoing |
| | CT-26 | s.c. | BALB/c | Yes | Yes | Yes | Yes | Yes |
| Fibrosarcoma | MC38 | s.c. | C57BL/6 | Yes | Yes | Yes | Yes | Yes |
| | WEHI-164 | s.c. | BALB/c | Ongoing | Ongoing | Ongoing | Ongoing | Ongoing |
| Kidney cancer | Renca | s.c. | BALB/c | Yes | Yes | Yes | Yes | Yes |
| | C1498 | s.c. | DBA/2 | Ongoing | Ongoing | Ongoing | Ongoing | Ongoing |
| Leukemia | L1210 | s.c. | C57BL/6 | Yes | Yes | Yes | Yes | Yes |
| | H22 | s.c./ortho | BALB/c | Yes | Yes | Yes | Yes | Yes |
| Liver cancer | KLN205 | s.c. | DBA/2 | Yes | Yes | Yes | Yes | Yes |
| | LL/2 | s.c./mets | C57BL/6 | Yes | Yes | Yes | Yes | Yes |
| Melanoma | A20 | s.c. | BALB/c | Yes | Yes | Yes | Yes | Yes |
| | E.G7-OVA | s.c. | C57BL/6 | Ongoing | Ongoing | Ongoing | Ongoing | Ongoing |
| Lymphoma | EL4 | s.c. | DBA/2 | Yes | Yes | Yes | Yes | Yes |
| | L5178-R | s.c. | DBA/2 | Yes | Ongoing | Ongoing | Ongoing | Ongoing |
| Mastocytoma | P338D1 | s.c. | C57BL/6 | Yes | Ongoing | Ongoing | Ongoing | Ongoing |
| | P815 | s.c. | DBA/2 | Ongoing | Ongoing | Yes | Yes | Yes |
| Melanoma | B16-BL6 | s.c. | C57BL/6 | Yes | Yes | Yes | Yes | Yes |
| | B16-F10 | s.c./ortho/mets | C57BL/6 | Yes | Yes | Yes | Yes | Yes |
| Myeloma | S91 | s.c. | DBA/2 | Ongoing | Ongoing | Ongoing | Ongoing | Ongoing |
| | MPC-11 | s.c. | BALB/c | Yes | Ongoing | Ongoing | Ongoing | Ongoing |
| Neuroblastoma | Neuro-2a | s.c. | A/J | Ongoing | Ongoing | Ongoing | Ongoing | Ongoing |
| Pancreatic cancer | Pan02 | s.c. | C57BL/6 | Ongoing | Yes | Yes | Yes | Yes |
| Plasmacytoma | J558 | s.c. | BALB/c | Ongoing | Ongoing | Ongoing | Ongoing | Ongoing |
| Prostate cancer | RM-1 | s.c. | C57BL/6 | Yes | Ongoing | Yes | Yes | Yes |

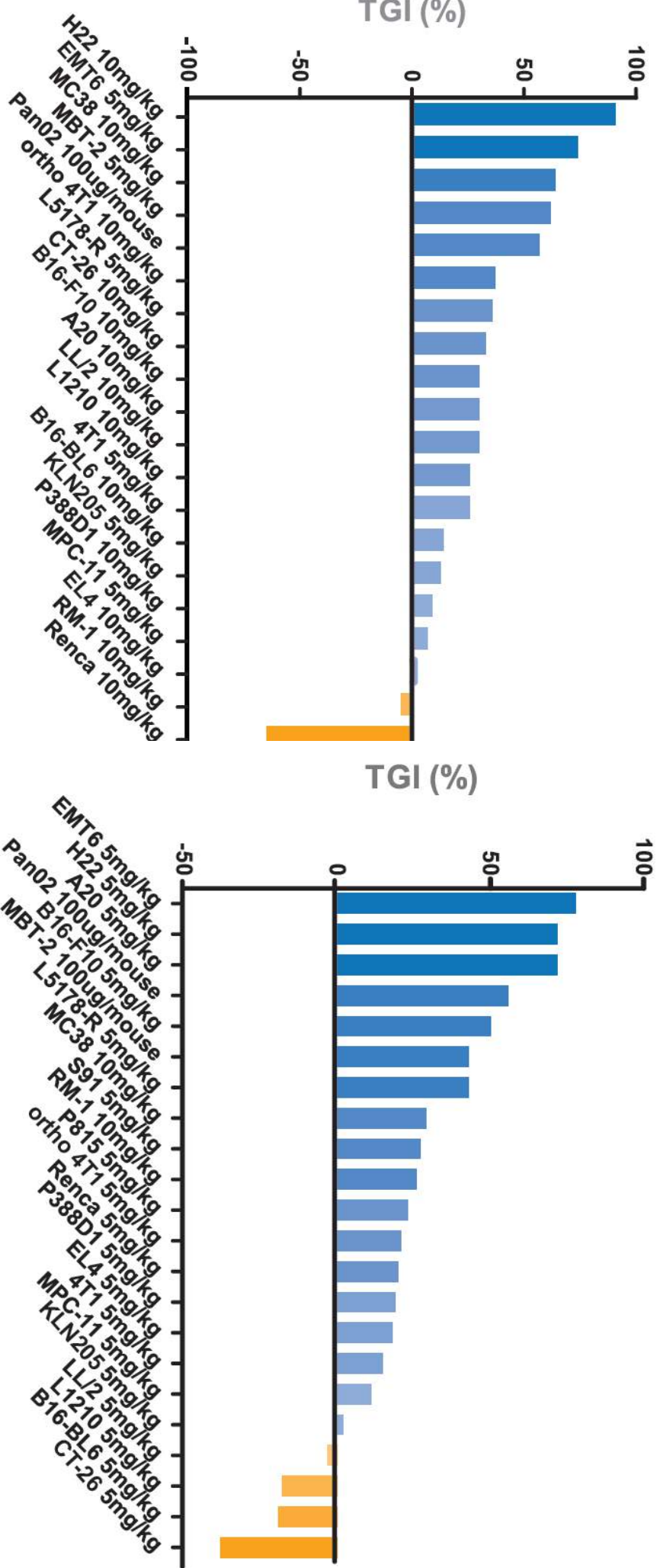


Anti-PD-1/PD-L1 Benchmarking

aPD-1 (RMP1-14)

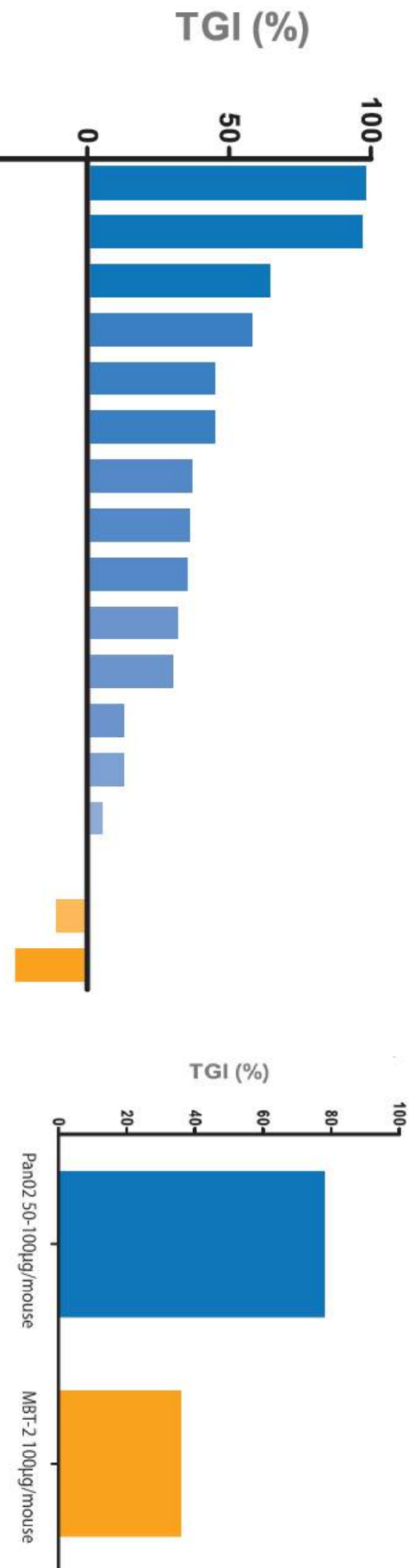


aPD-L1 (10F.9G2)



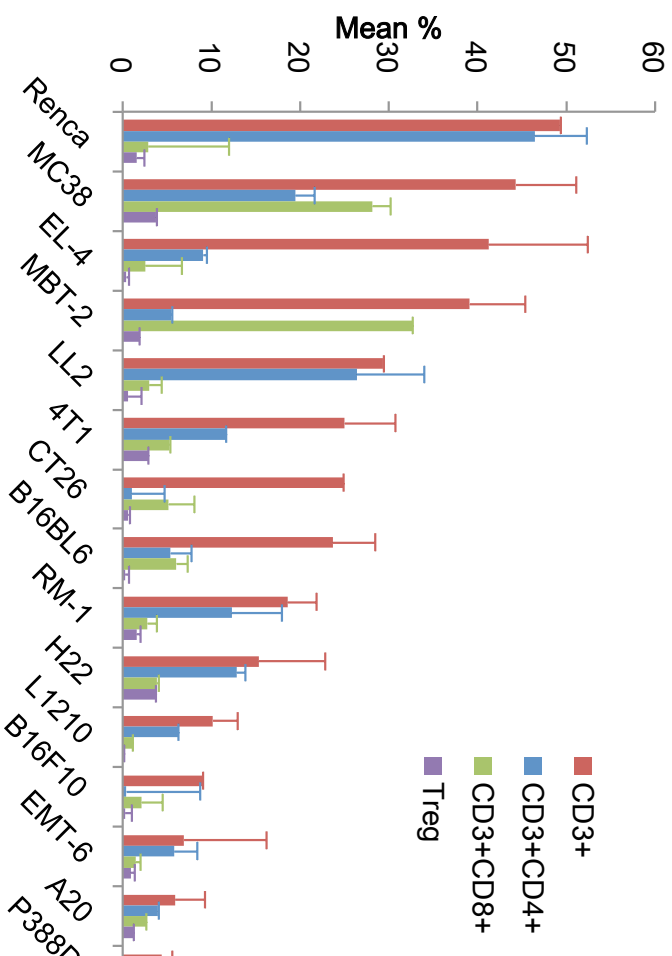
Anti-CTLA-4 Benchmarking

- Efficacy evaluation of aCTLA-4 (9D9) in syngeneic models
- Efficacy evaluation of aCTLA-4 (9H10) in syngeneic models

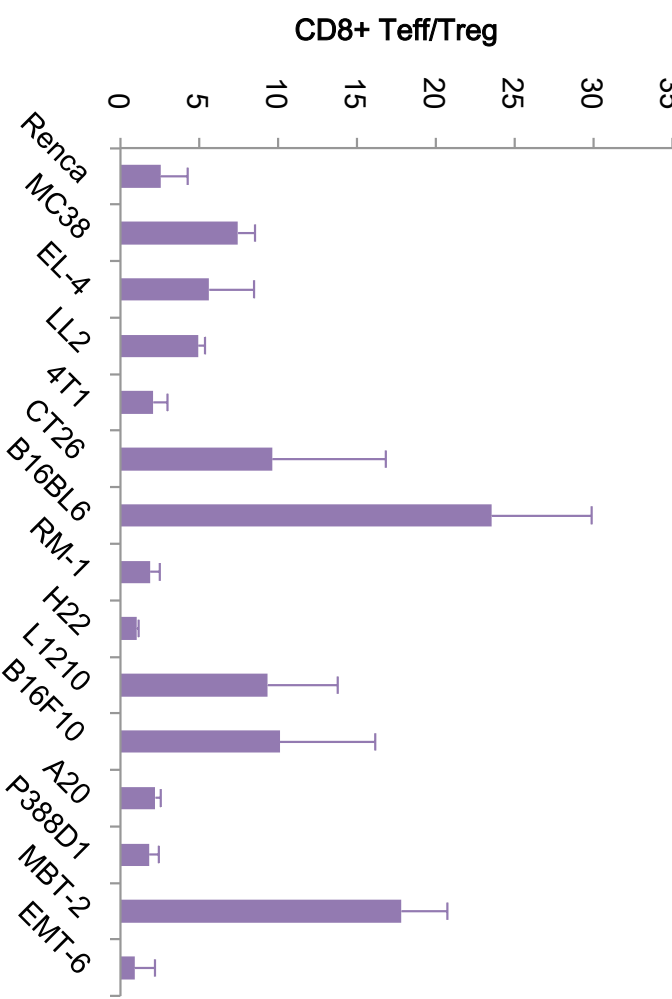


Base Line Immuno phenotyping

T Cell



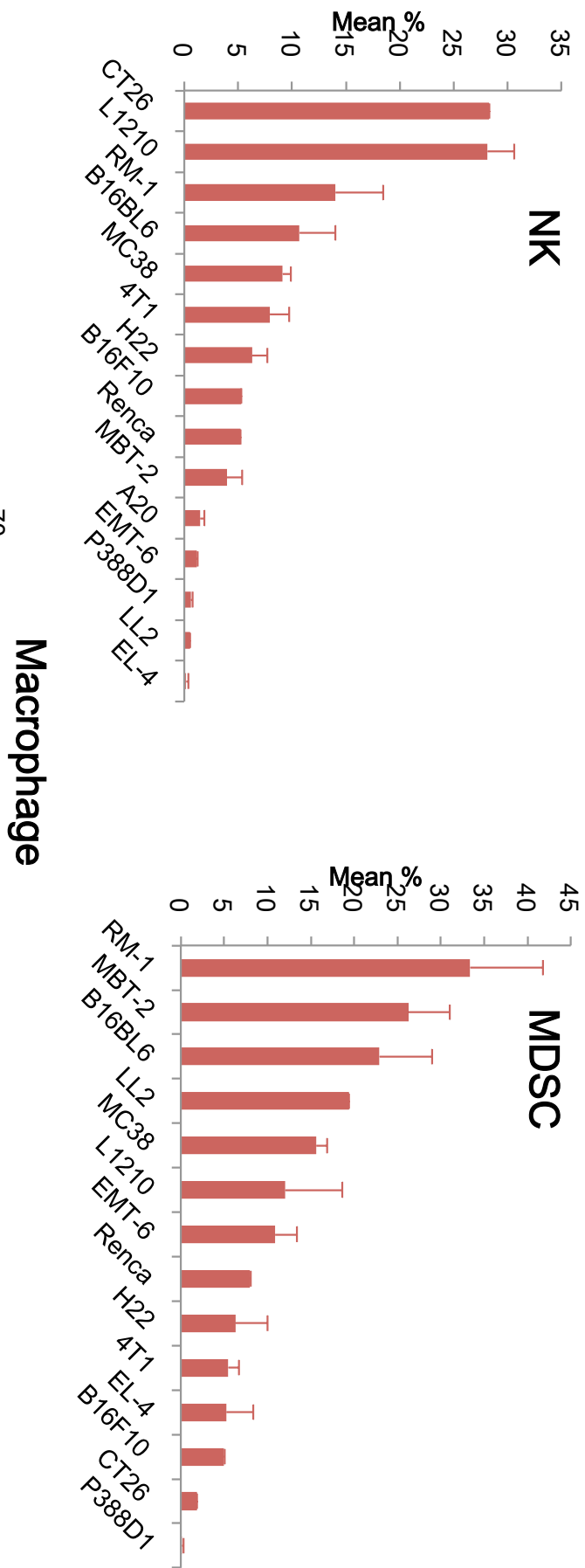
$T_{\text{eff}}/T_{\text{reg}}$



Depletion of CD8+ promotes MC38 tumour growth



Base Line Immuno phenotyping



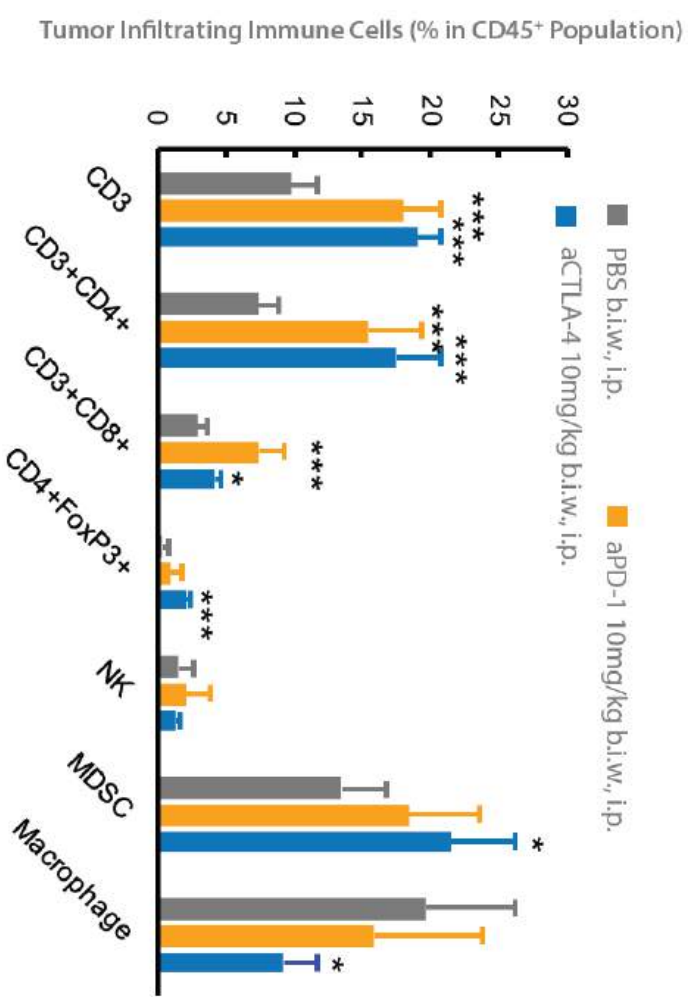
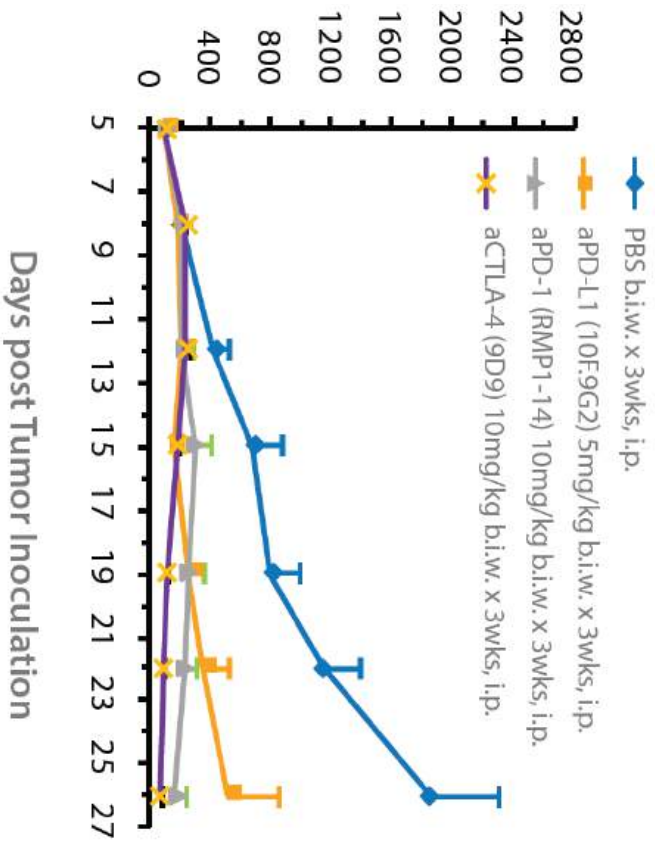


CrownBio
CONNECTING SCIENCE TO PATIENTS

H22 Checkpoint Antibodies Response & immunophenotyping

Highly sensitive to anti-CTLA-4, PD-1, and PD-L1 therapy

H22 tumor on Day 21: 2 days post 5th dose



| Treatment | Tumor Size (mm ³) on Day 26 | T/C Value (%) on Day 26 | p value |
|-------------------------|---|-------------------------|---------|
| PBS | 1843 ± 466 | -- | -- |
| aPD-L1 (10F.9G2) 5mg/kg | 520 ± 340 | 28 | 0.051 |
| aPD-1 (RMP1-14) 10mg/kg | 165 ± 73 | 9 | 0.007 |
| aCTLA-4 (9D9) 10mg/kg | 56 ± 9 | 3 | 0.005 |



CrownBio
CONNECTING SCIENCE TO PATIENTS

Oncology Knowledge Databases



OncoExpress****



- The world's first commercial database dedicated to mouse cancer models

- Free online access to search **Syngeneics**, **GEMM**, **MDX** (**Mu**Prime****), **Hu**GEMM**™**

- Make an informed decision by searching models based on gene expression, mutational status, gene fusions, etc. across our unique collection of mouse cancer models
- Wide variety of data compiled including model background, mouse strain, histopathology, genomic profiling (RNAseq), SoC, and immuno-profiling (infiltrate immune cells, cytokine profile, response to checkpoint inhibitors, etc.)



Hot Spot Mutations in Murine Tumors (partial list)

| MOD EL | GEN E | TRANSCRI PT | mRNA_P OS | CDS_P OS | RE F | AL T | DEPTH(REF:A LT) | AMINO_ACID_CHA NGE | CONFIDEN CE | MUTATIO NTY | Human Gene | Human protein ID | Human Gene Position | |
|------------|------------|---------------------|--------------|-------------|---------|---------|--------------------|-----------------------|----------------|----------------------|----------------------|---------------------|---------------------------|-------|
| B16B L6 | Braf 87 | ENSMUST 00000024 | 958 | 790 | T | C | 27:16 | C264R | PASS | Missensemutat ion | BRAF | ENSP0000288 602 | C280 | |
| MC38 | Braf 87 | ENSMUST | | | | | | W487C | PASS | Missensemutat ion | BRAF | ENSP0000288 602 | W450 | |
| MC38 | Egfr 29 | ENSMUST | 000000203 | 3579 | 3307 | G | T | 24:5 | G1103C | PASS | Missensemutat ion | EGFR | ENSP0000275 493 | G1103 |
| A20 | Erbb 95 | ENSMUST | 000000582 | 1251 | 1058 | G | T | 0:2 | G353V | PASS | Missensemutat ion | ERBB2 | ENSP0000269 571 | E352 |
| H22 | Erbb 95 | ENSMUST | 000000582 | 3426 | 3233 | C | T | 45:10 | P1078L | PASS | Missensemutat ion | ERBB2 | ENSP0000269 571 | P1077 |
| L1210 | Erbb 95 | ENSMUST | 000000582 | 581 | 388 | G | A | 0:2 | A130T | PASS | Missensemutat ion | ERBB2 | ENSP0000269 571 | V129 |
| CT26 | Fgf1 27 | ENSMUST | 000000840 | 1046 | 320 | C | T | 99:16 | S107F | QD | Missensemutat ion | FGFR1 | ENSP0000393 312 | S140 |
| MC38 | Fgf3 11 | ENSMUST | 000001144 | 1741 | 1433 | G | T | 2:6 | C478F | PASS | Missensemutat ion | FGFR3 | ENSP0000339 824 | F485 |
| L1210 | Fgf4 52 | ENSMUST | 000000054 | 2517 | 2177 | C | T | 0:2 | A726V | PASS | Missensemutat ion | FGFR4 | ENSP0000292 408 | A729 |
| 4T1 | Flt3 24 | ENSMUST | 000000493 | 3213 | 2989 | G | A | 0:6 | G997R | PASS | Missensemutat ion | FLT3 | ENSP0000241 453 | - |



CrownBio
CONNECTING SCIENCE TO PATIENTS

Whole Genome Gene Fusion Analysis: 4T1 Model

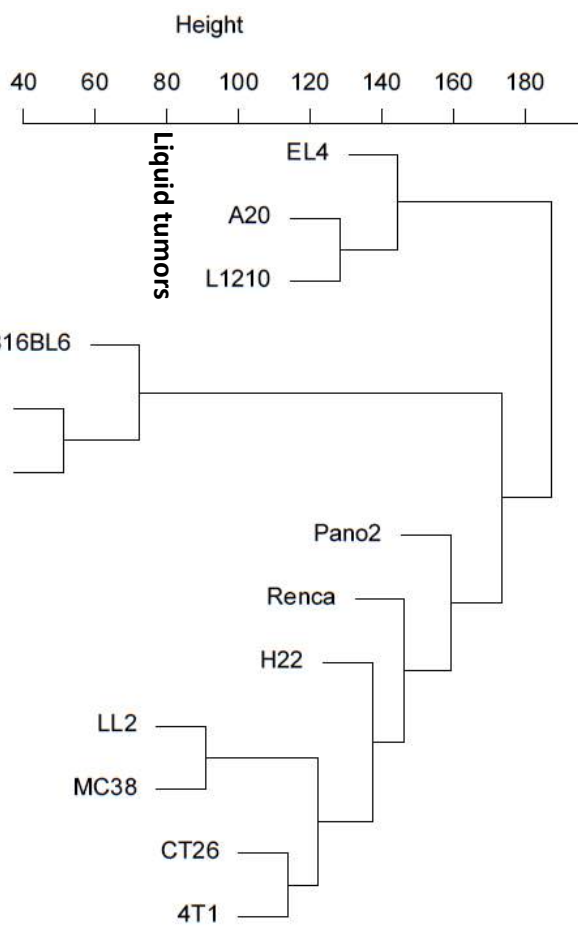
| | | | | up_gene | up_chr | up_strand | up_Genome_pos | up_loc | dw_gene | dw_chr | dw_strand | dw_Genome_pos | dw_loc | Span_reads_num | Junc_reads_num | Fusion_Type | down_fusion_part_frame-shift_or_not |
|---------|-------|---|----------|---------|------------|-----------|---------------|--------|----------|--------|-----------|---------------|--------|-----------------------|----------------|-------------|-------------------------------------|
| Ctla2b | chr13 | - | 60997599 | E | 4930486 | L24Rik | chr13 | - | 60956310 | E | 3 | 16 | 16 | INTRACHR-SS-OGO-GAP | frame-shift | | |
| D17H6S | chr17 | - | 35137158 | M | Errf1 | | chr4 | + | 1.5E+08 | M | 2 | 2 | 2 | INTERCHR-DS | NA | | |
| Eapp | chr12 | - | 55774558 | M | 1110002 | B05Rik | chr12 | - | 55747522 | E | 2 | 2 | 2 | INTRACHR-SS-OGO-1GAP | NA | | |
| F630111 | chr3 | - | 58957341 | M | P2y14 | | chr3 | - | 58920213 | E | 8 | 10 | 10 | INTRACHR-SS-OGO-GAP | NA | | |
| H2-M3 | chr17 | + | 37410855 | M | Olf755-ps1 | | chr17 | + | 37414914 | M | 2 | 5 | 5 | INTRACHR-SS-OGO-GAP | NA | | |
| Klhdc5 | chr6 | + | 1.47E+08 | M | Paip2b | | chr6 | - | 83763047 | M | 2 | 6 | 6 | INTRACHR-DS | NA | | |
| Kntc1 | chr5 | + | 1.24E+08 | E | Snmp35 | | chr5 | + | 1.25E+08 | E | 3 | 11 | 11 | INTRACHR-SS-OGO-10GAP | frame-shift | | |
| Ptms | chr6 | - | 1.25E+08 | M | Ptma | | chr1 | + | 88426037 | M | 2 | 2 | 2 | INTERCHR-DS | inframe-shift | | |
| Sema4d | chr13 | - | 51800322 | E | Gm1544_0 | | chr13 | - | 51796409 | M | 2 | 4 | 4 | INTRACHR-SS-OGO-GAP | inframe-shift | | |
| Vav3 | chr3 | + | 1.09E+08 | E | Chst7 | | chrX | + | 19674091 | E | 1 | 1 | 1 | INTERCHR-SS | NA | | |
| Znf1 | chr8 | + | 1.14E+08 | E | Zfp1 | | chr8 | + | 1.14E+08 | E | 1 | 1 | 1 | INTRACHR-SS-OGO-GAP | NA | | |



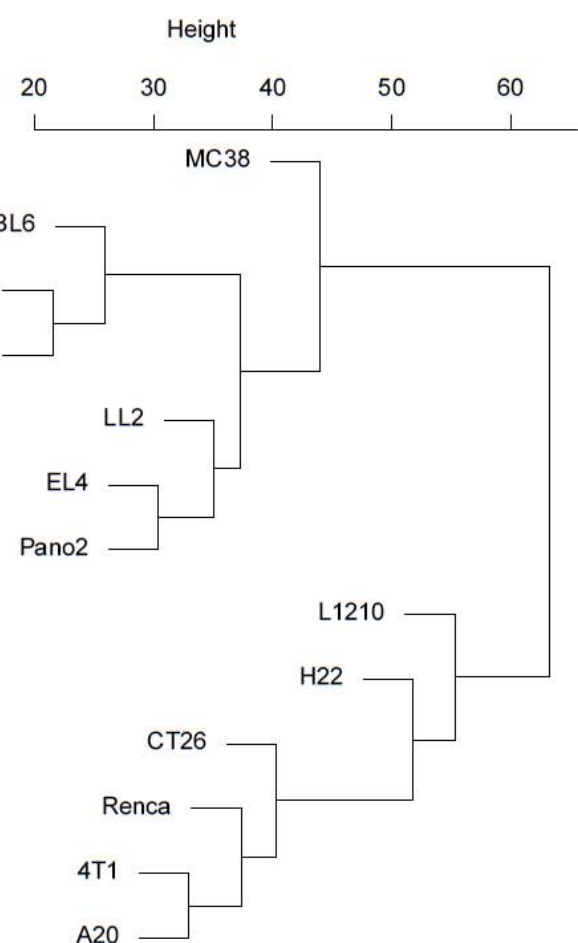
CrownBio
CONNECTING SCIENCE TO PATIENTS

Tumor Models Clustering by Gene Expression and Mutation

Cluster Dendrogram



Cluster Dendrogram



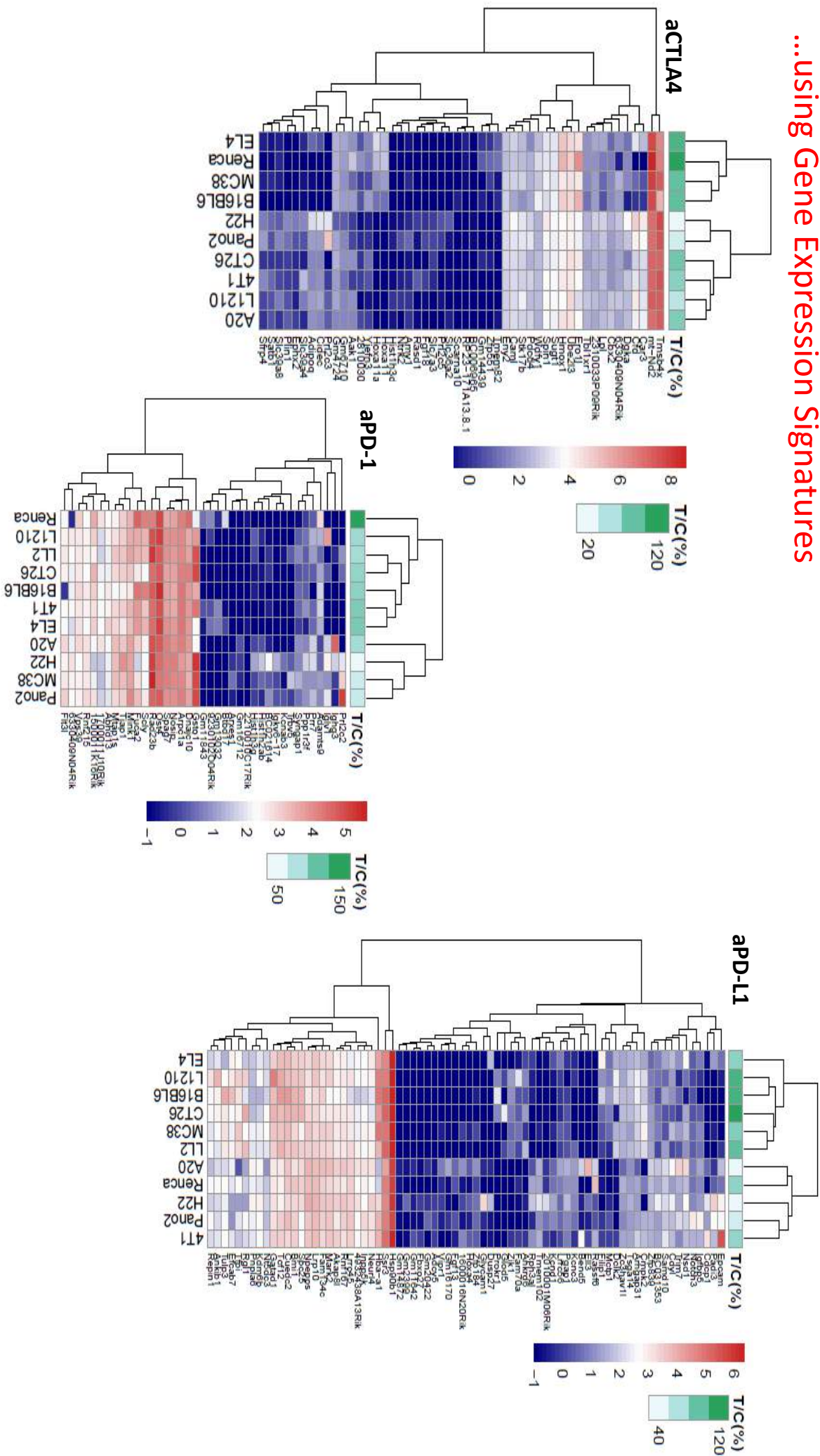
By Expression

By Mutation



CrownBio
CONNECTING SCIENCE TO PATIENTS

...using Gene Expression Signatures



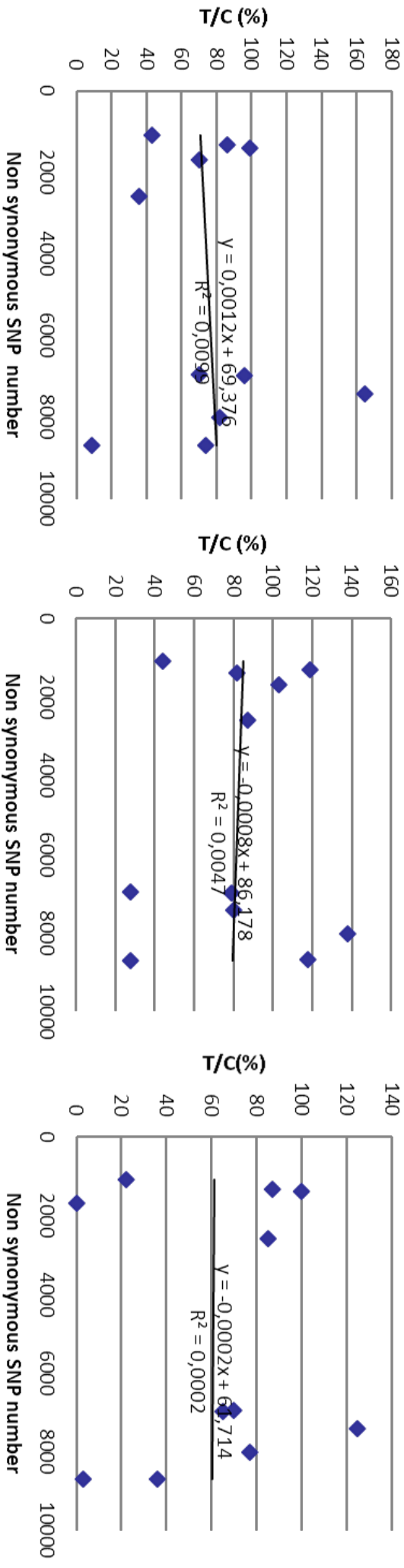
Efficacy Prediction of Immune Checkpoint Inhibition (I)



CrownBio
CONNECTING SCIENCE TO PATIENTS

Efficacy Prediction of Immune Checkpoint Inhibition (II)

...based on mutational load
...DNA repair gene mutations



No correlation was found...



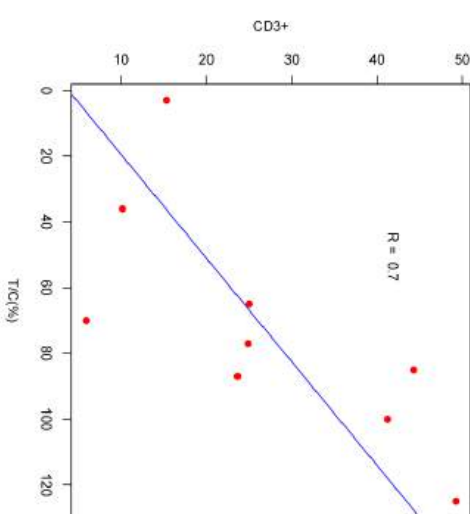
CrownBio
CONNECTING SCIENCE TO PATIENTS

Efficacy Prediction of Immune Checkpoint Inhibition (III)

...based on base line Immune Cells data

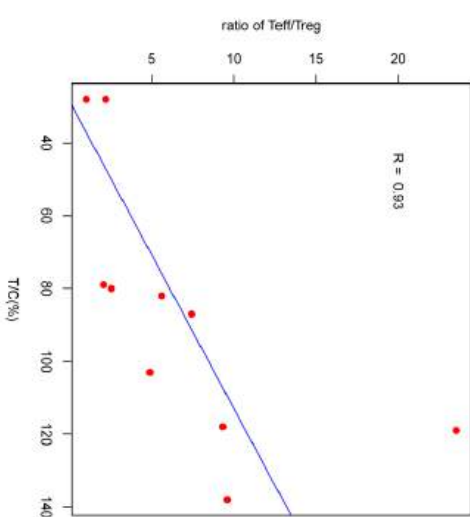
| FACS | aCTLA4 pvalue | aCTLA4 cor | aPD1 pvalue | aPD1 cor | aPDL1 pvalue | aPDL1 cor |
|--------------------|--------------------|--------------|-------------|--------------|-----------------|--------------------|
| CD3+ | 0.043253968 | 0.7 | 0.22755151 | 0.419454825 | 0.82820248 | 0.079027721 |
| CD3+CD4+ | 0.643639771 | 0.183333333 | 0.973408064 | -0.012158111 | 0.373561333 | -0.316110883 |
| CD3+CD8+ | 0.775628307 | 0.116666667 | 0.578406145 | -0.200608829 | 0.614067751 | 0.182371663 |
| Treg | 0.743540564 | -0.133333333 | 0.326657258 | -0.34650616 | 0.069155844 | -0.595747433 |
| ratio of Teff/Treg | 0.3125 | 0.383333333 | 0.626123419 | 0.176292608 | 9.60E-05 | 0.930095482 |
| NK | 0.46299052 | -0.283333333 | 0.789234533 | -0.097264887 | 0.072785937 | 0.589668377 |
| MDSC | 0.708068783 | 0.15 | 0.72525014 | -0.127660164 | 0.22755151 | 0.419454825 |
| Macrophage | 0.555952381 | 0.285714286 | 0.977546655 | 0.011976263 | 0.055884726 | 0.694623232 |

aCTLA4 (P-value = 0.0433)



Correlation trend was found...

aPDL1 (P-value = 9.6e-05)



- PD, model selection, rational combination approach but biomarker?



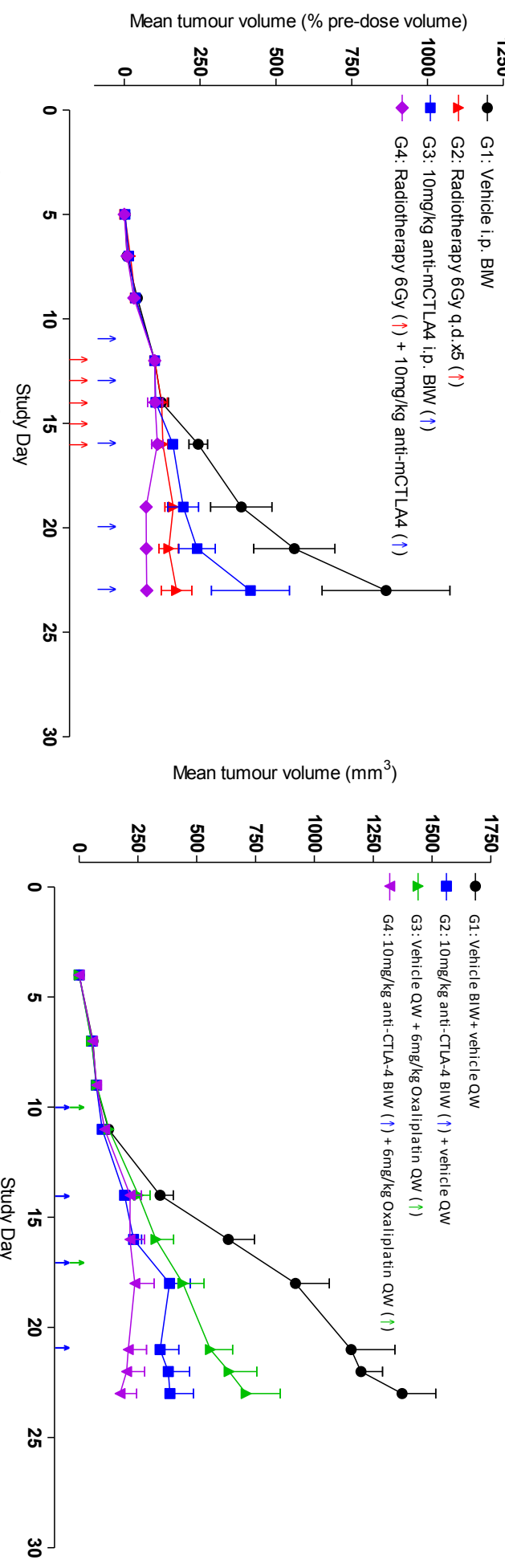
Combination with anti-mCTLA-4 (CT26)

CrownBio
CONNECTING SCIENCE TO PATIENTS

Induction of ICD:

Combination immunotherapy (anti-mCTLA-4) and radiotherapy (RT; hypofractionated IGMI) or Oxaliplatin was assessed alone, and in combination in BALB/c mice bearing subcutaneous CT26 allografts.

CT26 *in vivo* response to combination dosing of anti-mCTLA-4 + RT

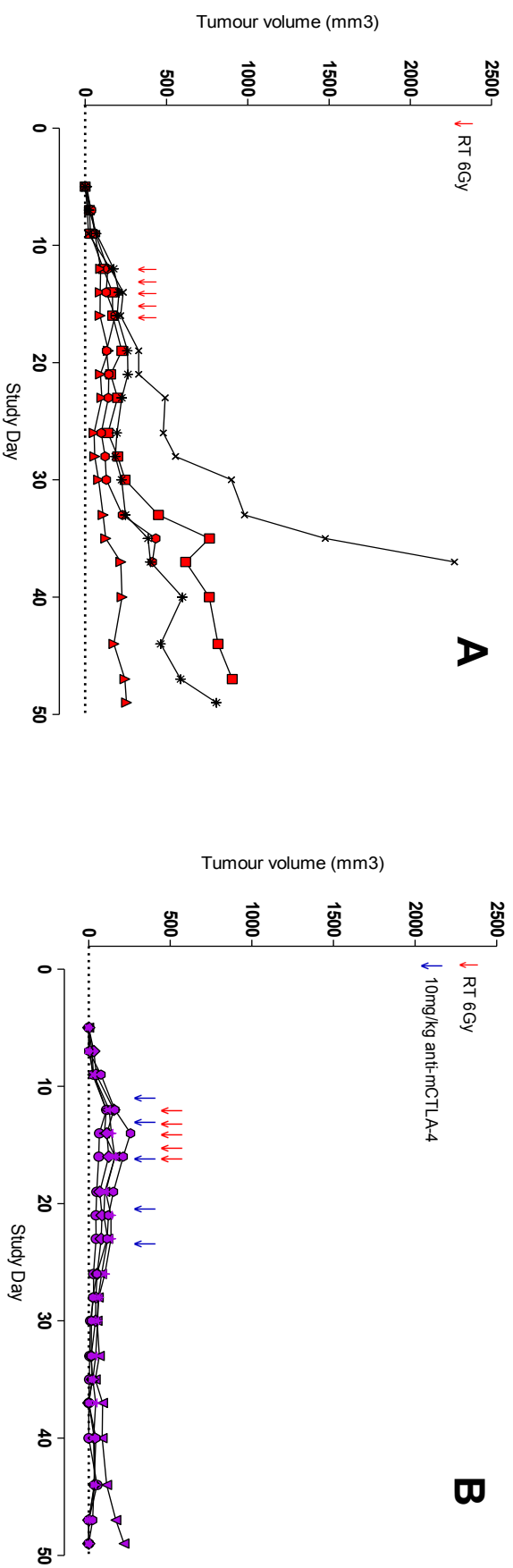


McKenzie et al AACR 2016, New Orleans

- Anti-mCTLA-4 and ICD monotherapy results in a statistically significant reduction in tumour growth ($p<0.05$) compared with vehicle treatment.
- Anti-mCTLA-4 therapy in combination with radiotherapy resulted in statistically significant additive reduction in tumour growth ($p<0.05$ Two-way ANOVA) versus anti-mCTLA-4 and RT monotherapies.

Long term combination effect (CT26)

CT26 *in vivo* outgrowth following A. RT treatment and B. anti-mCTLA-4 + RT



McKenzie et al AACR 2016, New Orleans

- Anti-mCTLA-4 and RT combination treated CT26 tumours, regression continued following cessation of treatment with a delay in tumour growth observed in comparison to RT alone.
- Markers of ICD (Calreticulin & HMGB1) TBD

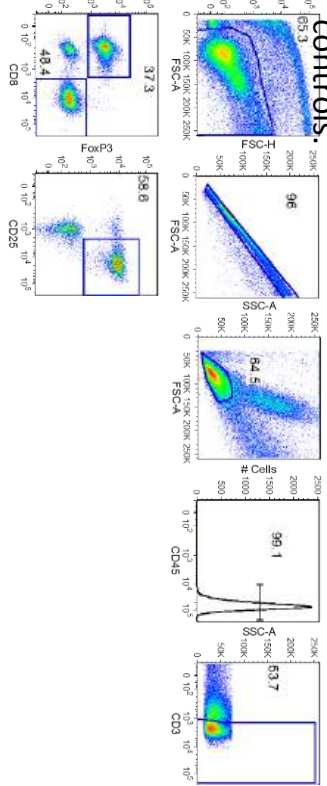


Increased CD8+ T cells (CT26)

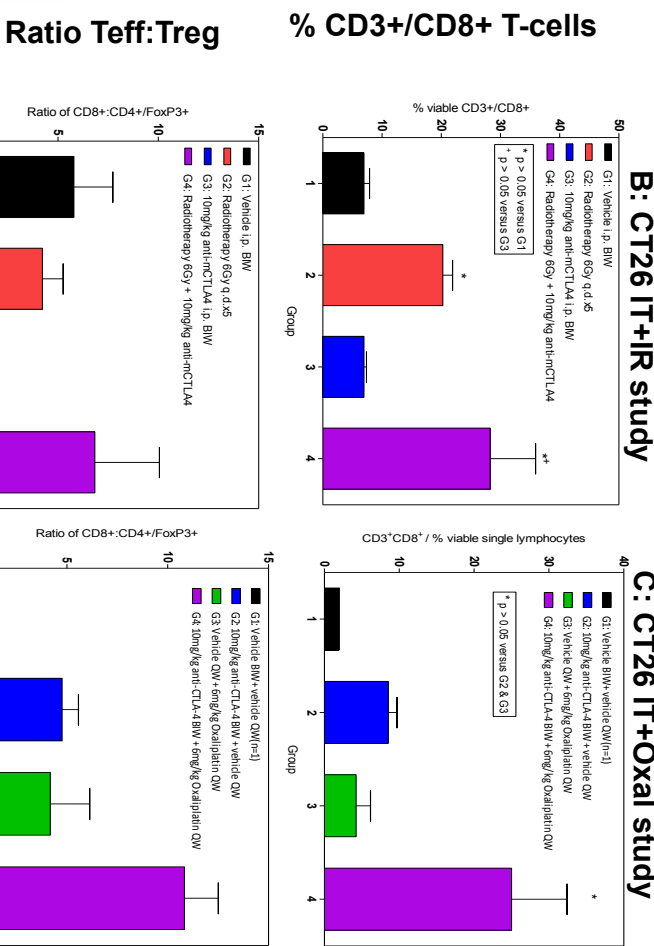
CrownBio
CONNECTING SCIENCE TO PATIENTS

Cytotoxic T-cells (Teff; CD3+/CD8+) and Treg (CD4+/CD25+/FoxP3+) tumour infiltration was assessed at day 23 in by FACS in CT26 tumours following treatment with immunotherapy (anti-mCTLA-4) and ICD alone and in combination

Representative flow cytometry plots: A-D.: Selection of single, viable lymphocytes. E.-F. CD4 vs CD8 T cells. F.-G. CD4+CD25+FoxP3+ T regulatory cells. Gating strategy was performed based on FMO



- Significant increase in CD8+ T-cells for both ICD and IT+ICD compared with vehicle control and versus IT alone for the IT+ICD group.
- Trend in increasing CD8+ T-cells for the IT+RT versus RT alone (which may be driving the additive efficacy seen in this treatment group) and significance for IT+Oxal.
- Treat larger sized tumours TBD



McKenzie et al AACR 2016, New Orleans

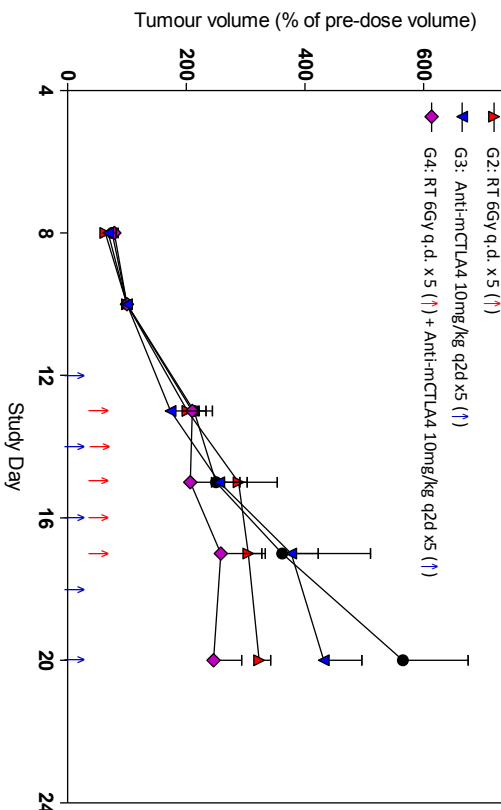


CrownBio
CONNECTING SCIENCE TO PATIENTS

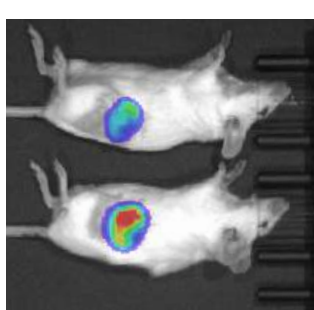
Bioluminescent breast carcinoma cell line 4T1-lux, metastasizes from the MFP > lung, lymph, liver and brain; and from S.C. site to the lung. Metastasis can be assessed by terminal ex vivo imaging.
The effect of monotherapy/combination therapy with 10mg/kg anti-mCTLA-4 i.p. q2d. (↑) and radiotherapy 6Gy qdx5 (↗) on tumour growth is detailed below.

In vivo response to combination dosing of anti-mCTLA-4 + RT

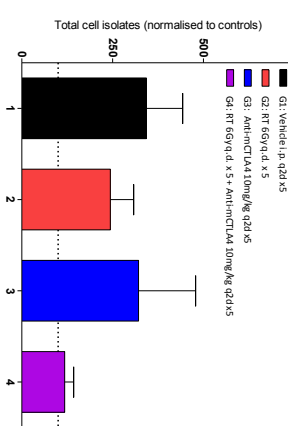
Tumour volume (% of pre-dose volume)



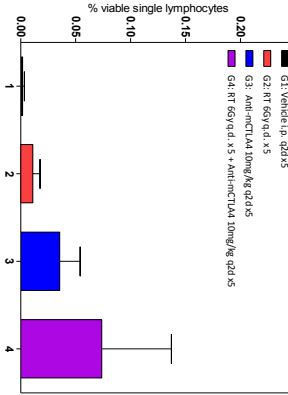
Ex vivo BLI of metastatic lung lesions from ex vivo tumour growth



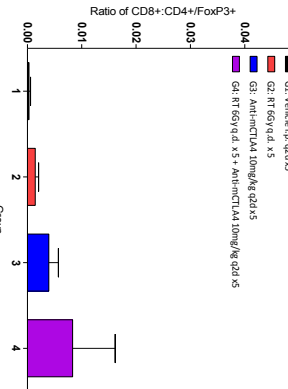
Whole lung total cell isolates



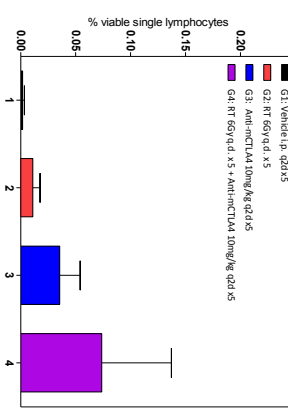
% CD3+/CD8+ T-cells



Ratio Teff:Treg



Flow cytometry analysis of 4T1 metastatic lung tumour



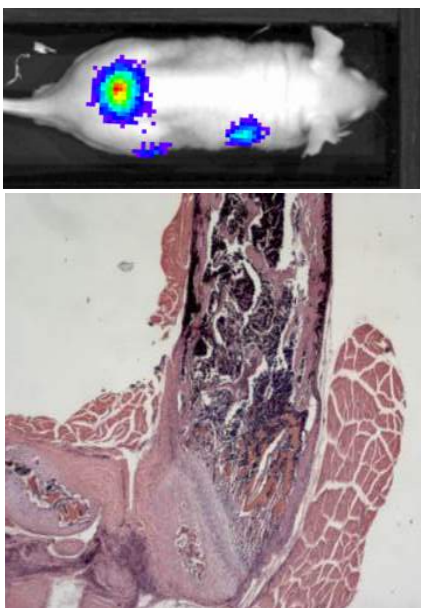


Mu-lux models under development

Ongoing

- Establishment at sc site ongoing for all syngeneic lines
- Transduction of remaining panel ongoing
- Bioluminescent syngeneic models, sc versus orthotopic ongoing for Pan02, H22, RM-1
- Metastasis assessment at end stage
- Experimental/seeding metastatic model development e.g. B16-F10

Bioluminescent B16-F10-lux mouse melanoma cells metastasise to bone following intracardiac inoculation. Metastasis can be assessed by terminal *ex vivo* imaging.

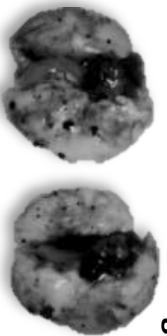


In-life BLI Histological confirmation of
immune cell infiltration quantification &
baseline data with FACS, Luminex, IHC

B16-F10-lux cells injected i.v. metastasise to the lungs

- Validation with immuno-therapeutics and combinations

Quantified by direct evaluation of macroscopic tumour deposits and *ex vivo* bioluminescent imaging.





CrownBio
CONNECTING SCIENCE TO PATIENTS

New Murine Models

- Syngeneic-Efficacy/PD
- MuPrime

Global I/O Platform Technologies

CrownBio
CONNECTING SCIENCE TO PATIENTS

- I/O CAR-T
- MiXeno
- PDX

- Advanced I/O
- HuGEMM
- HSC-PDX



CrownBio
CONNECTING SCIENCE TO PATIENTS

Overview of MuPrime Technology

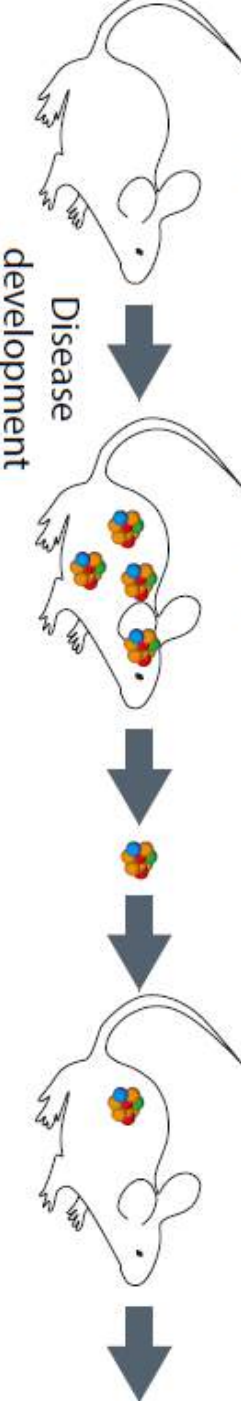
Procure congenic
GEMM/carcinogen
induced model

Autopsy
Biopsy
Imaging

Disease
development

MuPrime: Allograft to
syngeneic recipients

MuPrime Library

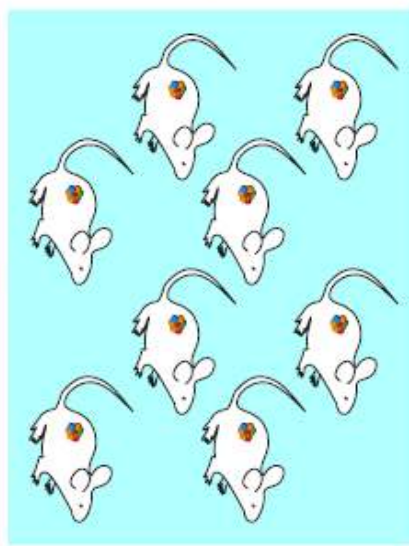
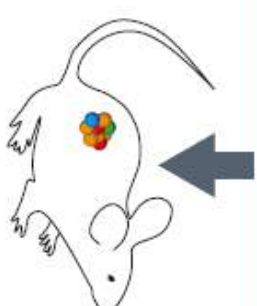


Annotations
Mouse information
Diagnosis
Treatment/prognosis
Genomic profiling

IHC staining
Primary Cell culture
Q.C.

Banking

MuTissue™
MuBank™



Efficacy study:
Targeted therapy
Chemotherapy
Immunotherapy

GEMM allografts for advanced I/O studies

Summary of MuPrime Models

| MuPrime ID | Cancer Type | Mutations/Carcinogen | Strain Background | Tumor Progression | MuPrime Setup | MuPrime Validation | Efficacy Ready? |
|---|------------------------------|--|-------------------|-------------------|---------------|--------------------|-----------------|
| Traditional GEMM-Derived MuPrime | | | | | | | |
| mPR6003 | Prostate | TRAMP (Pbsn-SV40TTG) | C57BL/6 | | Ongoing | Q3, 2016 | |
| mBR6004 | Breast | MMTV-PyVT TG | FVB/N | | Ready | | |
| mSK6005 | Skin squamous cell carcinoma | Apc ^{Min/+} | C57BL/6 | | Ready | | |
| mLY6043 | B cell lymphoma | IgH-Myc TG (Eμ Myc) | C57BL/6 | | Ready | | |
| mSA9003 | Sarcoma | P53 ^{-/-} | C57BL/6 | | Ready | | |
| mLY6041 | B cell lymphoma | KRAS(G12D); P53 ^{-/-} | C57BL/6 | | Ready | | |
| mLU6042, | Lung | KRAS(G12D); P53 ^{-/-} | C57BL/6 | | Ready | | |
| mLU6044, | | | | | | | |
| mLU6045 | | | | | | | |
| mCR6046 | Colon | KRAS(G12D); P53 ^{-/-} | C57BL/6 | | Ready | | |
| mLI6047 | Liver | KRAS(G12D); P53 ^{-/-} | C57BL/6 | | Ready | | |
| | Pancreatic | KRAS(G12D); P53 ^{-/-} | C57BL/6 | Ongoing | Q2, 2016 | | |
| | Prostate | KRAS(G12D); PTEN ^{Flx/Flx} | C57BL/6 | Ongoing | Q4, 2016 | | |
| | Ovarian | KRAS(G12D); PTEN ^{Flx/Flx} | C57BL/6 | Ongoing | Q3, 2016 | | |
| | Bladder | KRAS(G12D); PTEN ^{Flx/Flx} | C57BL/6 | Ongoing | Q3, 2016 | | |
| | Lung | KRAS(G12D); PTEN ^{Flx/Flx} | C57BL/6 | Ongoing | Q2, 2016 | | |
| | Glioblastoma | KRAS(G12D); PTEN ^{Flx/Flx} | C57BL/6 | Ongoing | Q3, 2016 | | |
| | Bladder | PTEN ^{Flx/Flx} ; P53 ^{-/-} | C57BL/6 | Ongoing | Q2, 2016 | | |
| | Prostate | PTEN ^{Flx/Flx} ; P53 ^{-/-} | C57BL/6 | Ongoing | Q4, 2016 | | |
| | Pancreatic | KRAS(G12D); P16 ^{-/-} | C57BL/6 | Ongoing | Q3, 2016 | | |
| | Lung | KRAS(G12D); P16 ^{-/-} | C57BL/6 | Ongoing | Q3, 2016 | | |



CrownBio
CONNECTING SCIENCE TO PATIENTS

MuPrime mBR6004

Parental GEMM strain

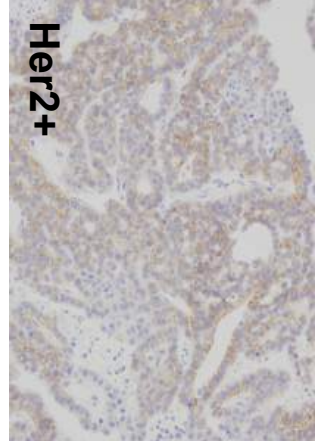
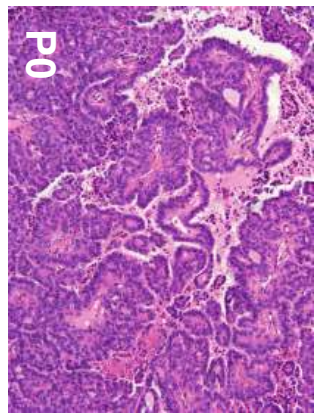
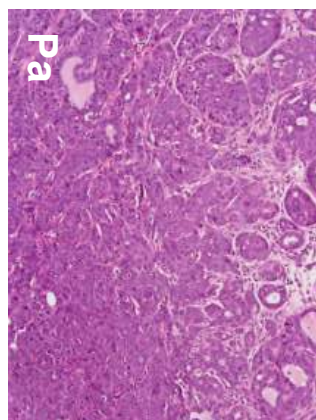
FVB/N-Tg (MMTV-PyVT)634Mul/Jnju

Strain background

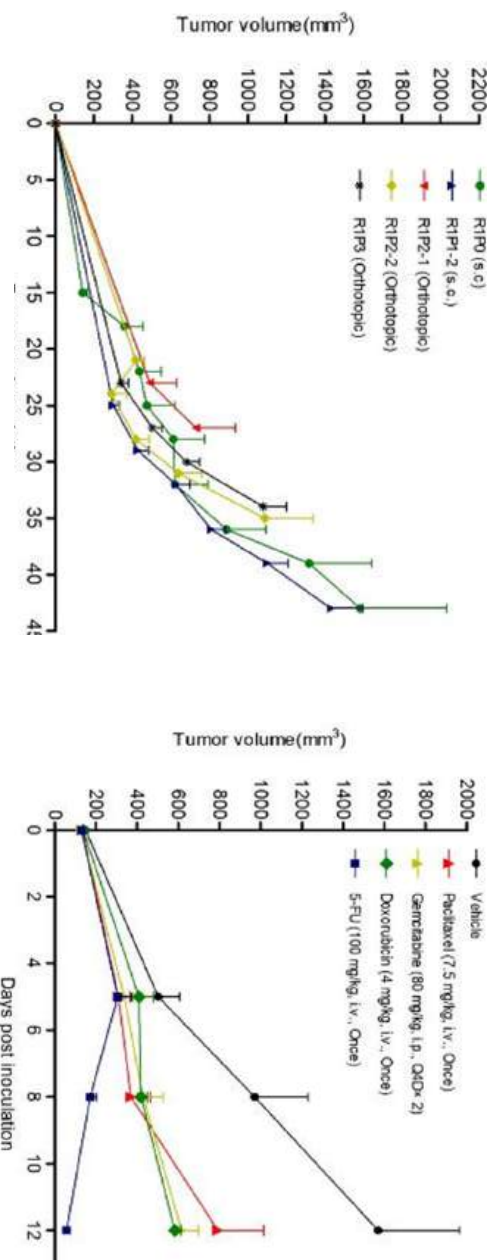
FVB/N

Pathology diagnosis

Breast cancer

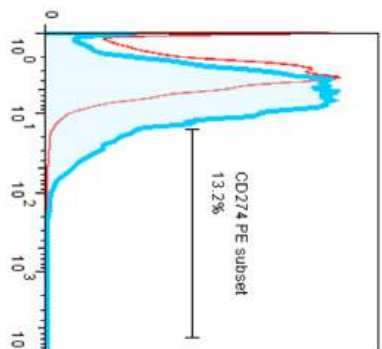


| | |
|---------------|-------------------------|
| EGFR | FS-insertion 14.31G->GA |
| ERBB2 | A130T |
| MET | I851M |
| KRAS | WT |
| BRAF | WT |
| AKT1 | WT |
| PIK3CA | WT |
| CTNNB1 | WT |
| PTEN | WT |

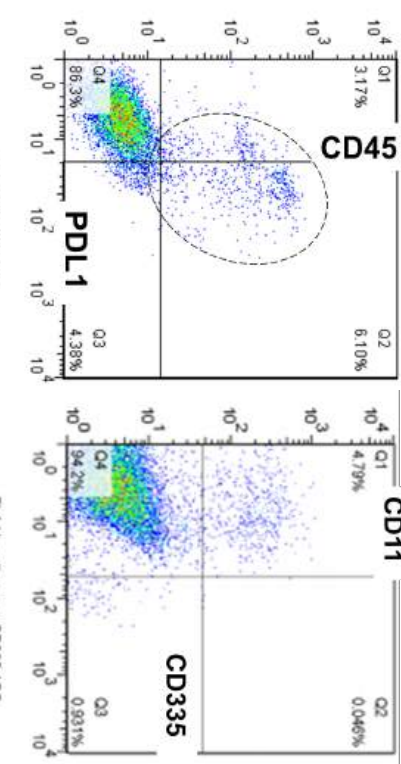


mBR6004 Immune Profiling and Response to Checkpoint Inhibitors

PD-L1 Expression



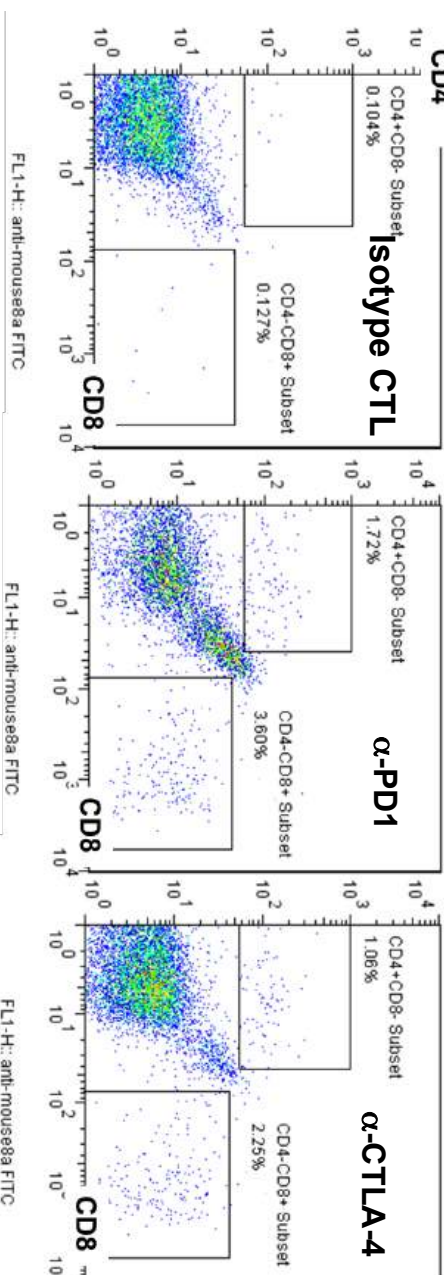
Baseline Infiltrating Immune Cells



Baseline Infiltrating NK/Neutrophils



Tumor-Infiltrating Lymphocytes upon Treatment



Efficacy & TIL Summary

| | TV (mm ³) | CD4% | CD8% |
|-------------|-----------------------|-------|-------|
| Isotype CTL | 829 | 0.104 | 0.127 |
| α-PD1 | 438 | 1.72 | 3.60 |
| α-CTLA-4 | 345 | 1.06 | 2.25 |



CrownBio
CONNECTING SCIENCE TO PATIENTS

Humanised Systems

Global I/O Platform Technologies

CrownBio
CONNECTING SCIENCE TO PATIENTS

- I/O CAR-T
- MiXeno
- HugEMM
- PDX

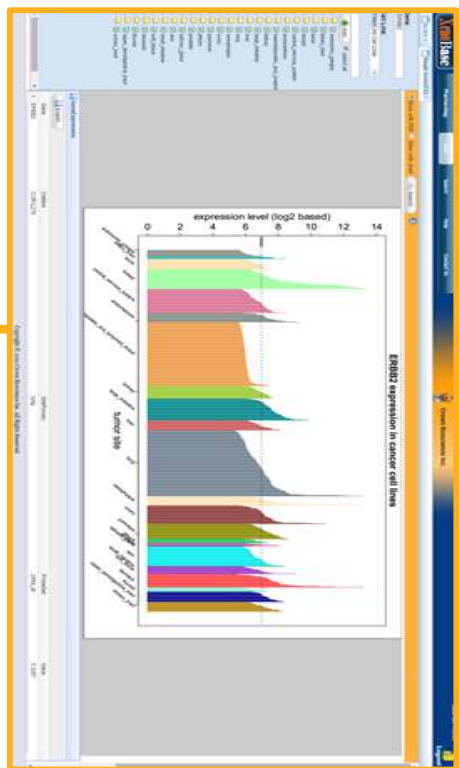
- Efficacy/PD
- Syngeneic-MuBase
- MuPrime

Advanced I/O



CrownBio
CONNECTING SCIENCE TO PATIENTS

Oncology Knowledge Databases



Onco**Express**

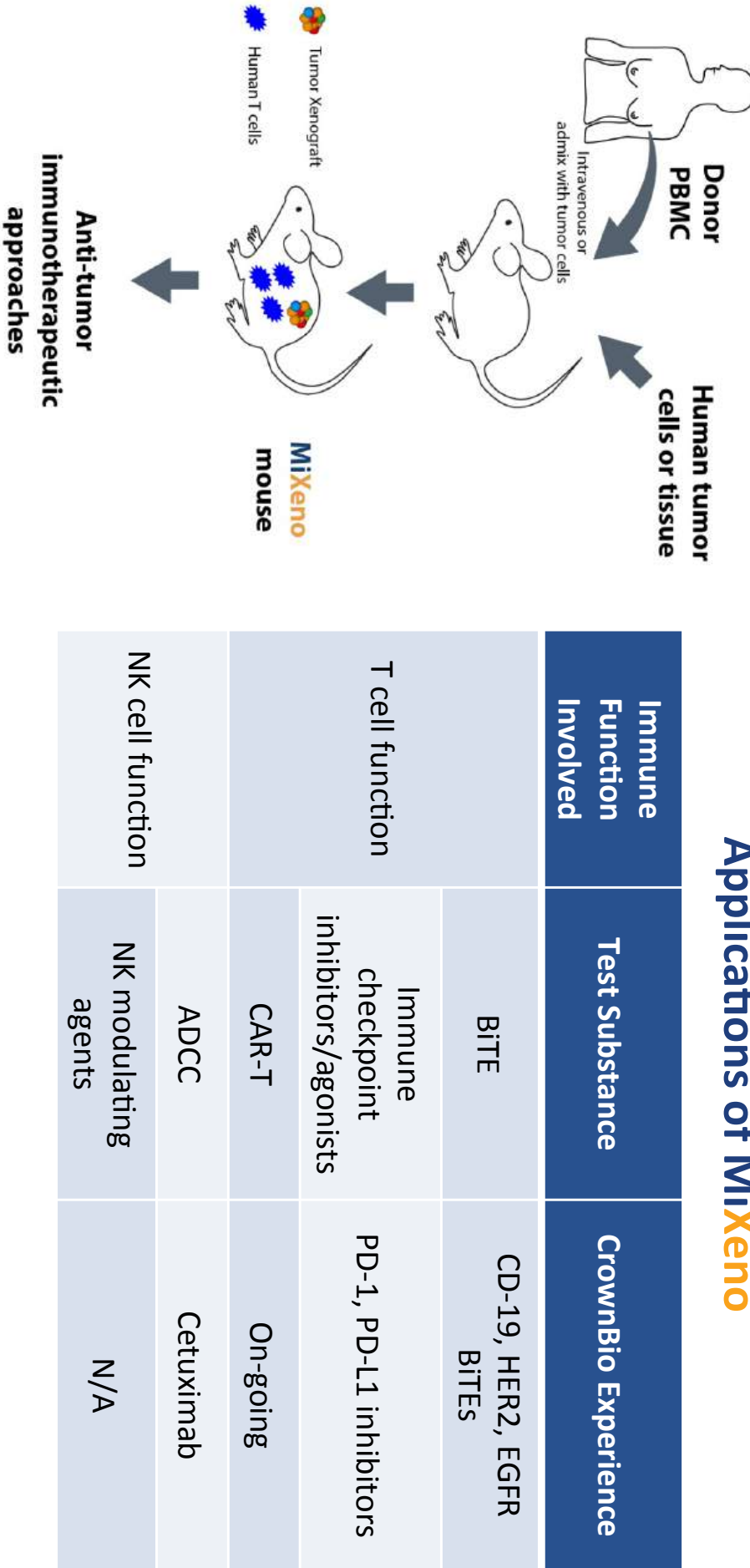
- Free online database for curated CDX models
- Over 2,000 cell lines available
- Combining public **profiling data** (gene expression, copy number and mutation) and proprietary *in vivo pharmacology data*
- Make an informed decision by searching based on gene mutation, amplification and expression, tumor growth *in vivo* and response to SoC treatments



CrownBio
CONNECTING SCIENCE TO PATIENTS

MiXeno Concept

Applications of MiXeno

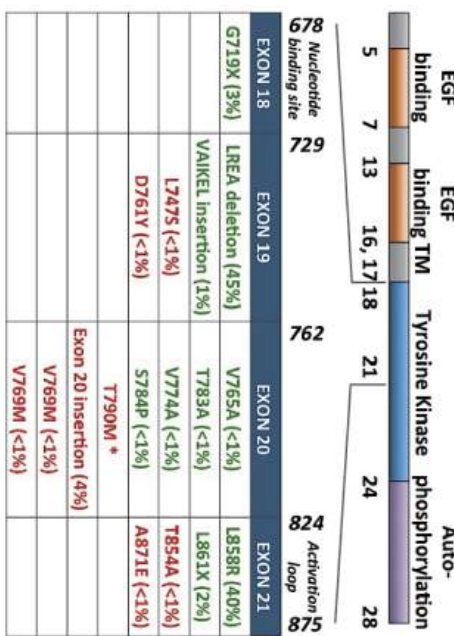


A fast and economic way to evaluate I/O therapies alone or in combination

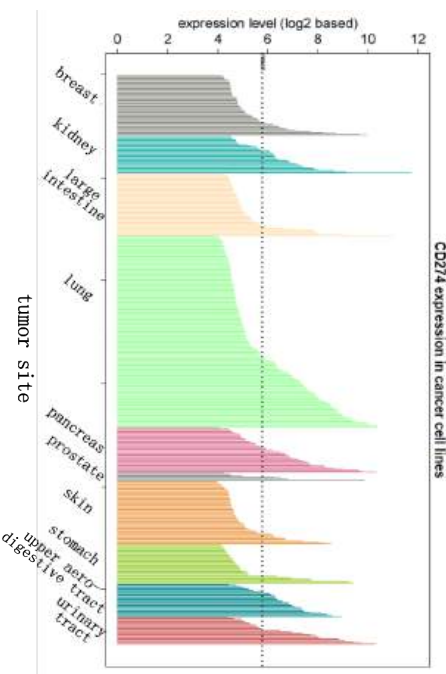
HCC-827 NSCLC model

- Somatic mutations in EGFR gene in NSCLC
- HCC-827 NSCLC adenocarcinoma cell line
- Harbours an activating EGFR mutation (del E746-A750)
- HCC-827 erlotinib resistant models generated with c-met amplification
- High PD-L1 expression (Xenobase & FACS)

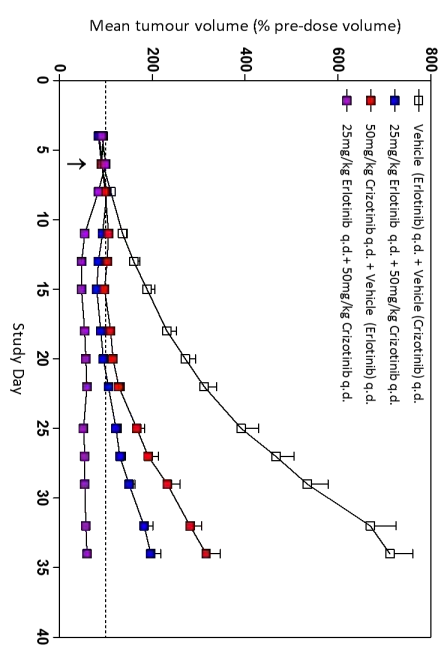
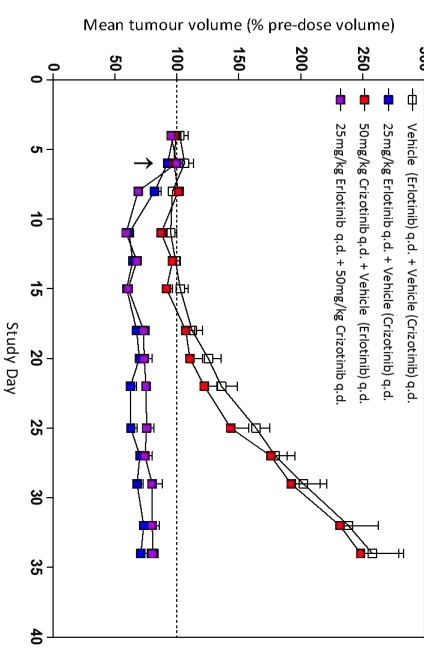
Somatic Mutations in the EGFR Gene



PD-L1 expression



HCC-827 WT model shows exquisite sensitivity to Erlotinib whereas as the resistant model shows c-met amplification and sensitivity to Crizotinib



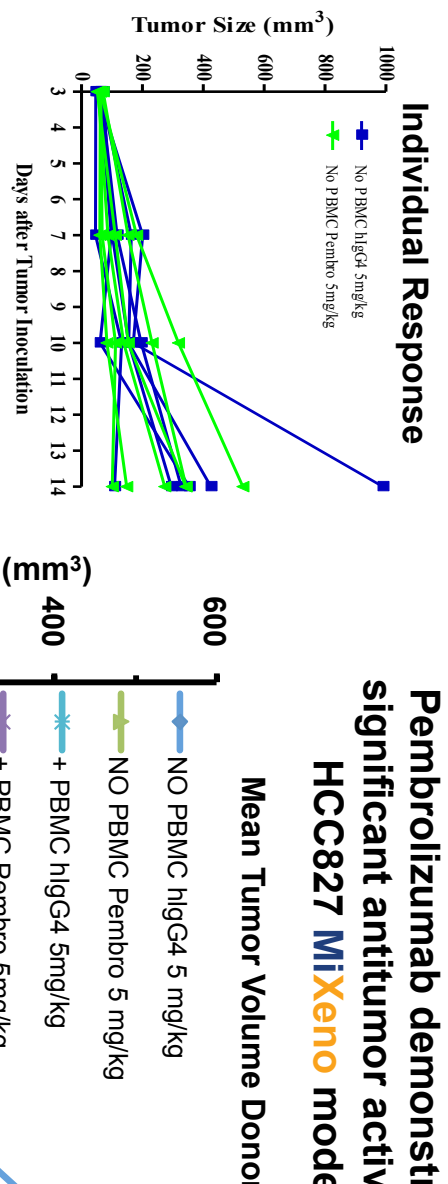


CrownBio
CONNECTING SCIENCE TO PATIENTS

HCC827 – MiXeno Model Anti-PD-1 Ab Antitumor Activity

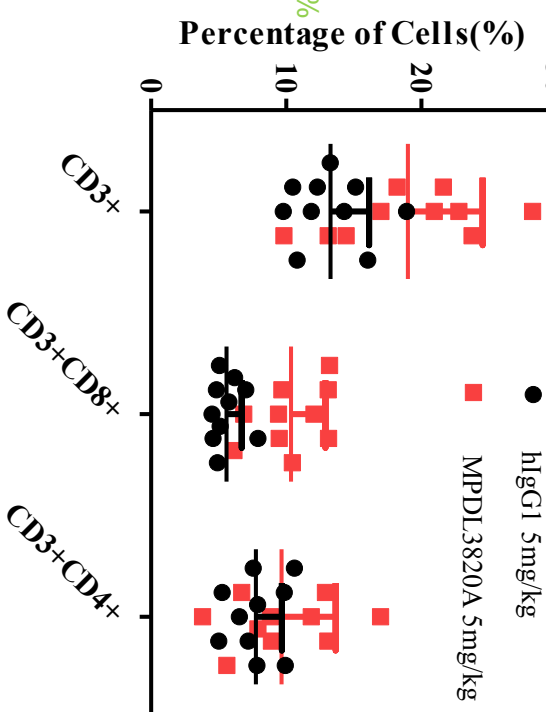
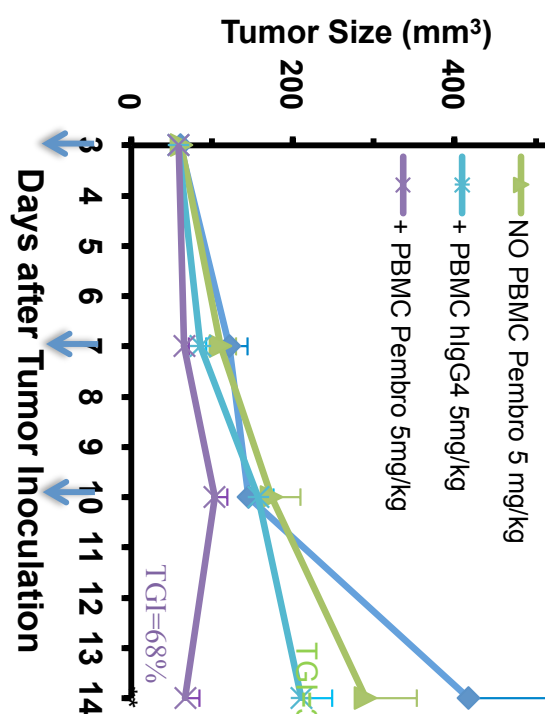
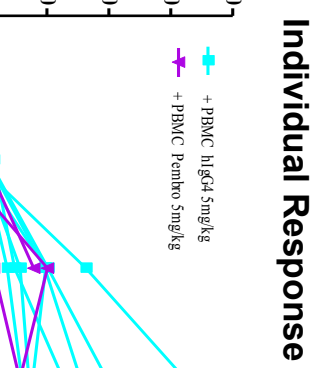
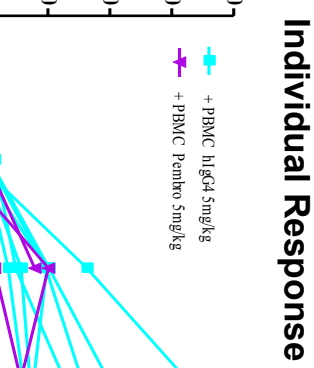
Pembrolizumab demonstrated significant antitumor activity in HCC827 **MiXeno** model

Mean Tumor Volume Donor A+B



Increased lymphocyte presence after treatment with anti-PD-L1 antibody

Blood



- Evaluation of combination & response in resistant model underway
- PDX models with ERGFR mutations



CrownBio
CONNECTING SCIENCE TO PATIENTS

Additional models/developments

Global I/O Platform Technologies

CrownBio
CONNECTING SCIENCE TO PATIENTS

- I/O CAR-T
- MiXeno
- PDX

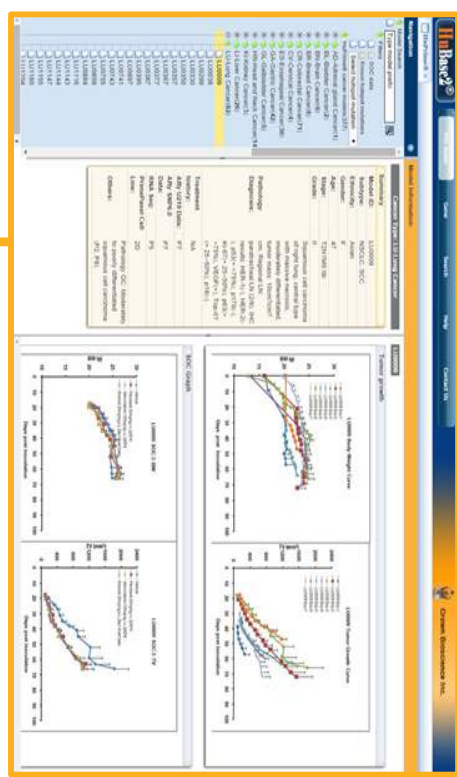
- Efficacy/PD
- MuPrime
- Syngeneic-MuBase

- Advanced I/O
- HuGEMM
- HSC-PDX



CrownBio
CONNECTING SCIENCE TO PATIENTS

PDX Oncology Knowledge Databases



OncоЕxpress

HuBase2®

HuBase

- **Free online database to access our curated >2500 PDX models**
- **Complete genomic annotation** (gene expression, copy number and mutation), **clinical and pharmacology data**
- Select models that match your criteria using: clinical information, diagnosis and pathology, whole genome gene expression profiling and copy number variation, Hotspot sequence mutation, key biomarker IHC information, tumor growth and SoC response curve

Summary: Strategies to induce anti-tumour immune response





CrownBio
CONNECTING SCIENCE TO PATIENTS

Thank you & acknowledgments

CBSD

Tommy Broudy
Jayant Thatte

CBNC

Leo Liu

PreClinOmics, a Crown Bioscience company.
7918 Zionsville Rd.
Indianapolis
Indiana
USA

CBUK

Rajendra Kumari*
Andrew McKenzie
Nektaria Papadopoulou

CBBJ
Henry Li*
Jie Cai
Sheng Guo
Annie An

CBTC

Qian Shi*
Juan Zhang
Davy Ouyang
Jinying Ning

Crown Bioscience Inc.
3375 Scott Blvd., Suite 108
Santa Clara
California
USA

Crown Bioscience (San Diego)
11011 Torreyana Road, Suite 150
San Diego
California
USA

Crown Bioscience North Carolina Inc.
David H Murdock Research Institute
Kannapolis
North Carolina
USA

Crown Bioscience Inc. (Taicang)
Science & Technology Innovation Park
No. 6 Beijing West Road
Taicang City
Jiangsu Province

Crown Bioscience Inc. (Beijing)
17F, No. 333, Sec. 1, Keelung Road
Xinyi District
Taipei City
Taiwan



Global capacity
>40,000 mice



CrownBio
CONNECTING SCIENCE TO PATIENTS

CrownBio Worldwide Operations

USA

Crown Bioscience Inc.

3375 Scott Blvd., Suite 108
Santa Clara, CA 95054

Tel: +1-855-827-6968

Fax: +1-888-882-4881

Crown Bioscience USA, NC (IIBR)

150 N Research Campus Drive
Kannapolis, North Carolina 28081

Tel: +1-704-250-2680

Fax: +1-704-250-2609

Crown Bioscience (San Diego)

11011 Torreyana Road, Suite 200
San Diego, CA 92121 Tel: +1-858-622-2900

TAIWAN

Crown Bioscience Inc. (Taiwan)

Light Muller Building
Changping Sector of Zhongguancun Science Park No.21
Huoju Street, Changping District
Beijing P.R. China 102200

Tel: +86-10-5633-2600 or 888-881-2246
Fax: +86-10-5633-2700

Crown Bioscience Inc. (Taicang)

Science & Technology Innovation Park
No.6 Beijing West Road, Taicang City
Jiangsu Province P.R. China 215400

Tel: +86-512-5387-9999

Fax: +86-512-5387-9801

CHINA

Crown Bioscience Inc. (Beijing)

Changping Sector of Zhongguancun Science Park No.21
Huoju Street, Changping District
Beijing P.R. China 102200

Tel: +86-10-5633-2600 or 888-881-2246

Fax: +86-10-5633-2700

EUROPE

Crown Bioscience UK Ltd.

Hillcrest, Dodgeford Lane, Belton
Loughborough LE12 9TE, UK
Tel: +44-870-166-623 Fax: +44-870-166-6233